

European Heart Journal - Cardiovascular Imaging

Global Longitudinal Active Strain Energy Density (GLASED): A Powerful Prognostic Marker in a Community-Based Cohort

--Manuscript Draft--

Manuscript Number:	EHJCI-D-23-01505R2
Full Title:	Global Longitudinal Active Strain Energy Density (GLASED): A Powerful Prognostic Marker in a Community-Based Cohort
Article Type:	Original Paper
Keywords:	contractance, contractility, contractile function, energy, heart failure, systolic function, stroke work
Corresponding Author:	David Hunter MacIver, MB, BS, MRCP, T(M), MD, EFESC Taunton and Somerset NHS Trust: Somerset NHS Foundation Trust Taunton, UNITED KINGDOM
Corresponding Author Secondary Information:	
Corresponding Author's Institution:	Taunton and Somerset NHS Trust: Somerset NHS Foundation Trust
Corresponding Author's Secondary Institution:	
First Author:	Nay Aung
First Author Secondary Information:	
Order of Authors:	Nay Aung David Hunter MacIver, MB, BS, MRCP, T(M), MD, EFESC Henggui Zhang Sucharitha Chadalavada Steffen E. Petersen
Order of Authors Secondary Information:	
Abstract:	<p>Background Identifying the imaging method that best predicts all-cause mortality, cardiovascular adverse events and heart failure risk is crucial for tailoring optimal management. Potential prognostic markers include left ventricular myocardial mass, ejection fraction, myocardial strain, stroke work, contraction fraction, pressure-strain product and a new measurement called global longitudinal active strain density (GLASED).</p> <p>Objectives This study sought to compare the utility of 23 potential left ventricular prognostic markers of structure and contractile function in a community-based cohort.</p> <p>Methods The impact of cardiovascular magnetic resonance image-derived markers extracted by machine learning algorithms was compared to the future risk of adverse events in a group of 44,957 UK Biobank participants.</p> <p>Results Most markers, including the left ventricular ejection fraction, have limited prognostic value. GLASED was significantly associated with all-cause mortality and major adverse cardiovascular events, with the largest hazard ratio, highest ranking and differentiated risk in all three tertiles ($P \leq 0.0003$).</p> <p>Conclusions GLASED predicted all-cause mortality and major cardiovascular adverse events better than conventional markers of risk and is recommended for assessing patient prognosis.</p>

Background

Identifying the imaging method that best predicts all-cause mortality, cardiovascular adverse events and heart failure risk is crucial for tailoring optimal management. Potential prognostic markers include left ventricular myocardial mass, ejection fraction, myocardial strain, stroke work, contraction fraction, pressure-strain product and a new measurement called global longitudinal active strain density (GLASED).

Objectives

This study sought to compare the utility of 23 potential left ventricular prognostic markers of structure and contractile function in a community-based cohort.

Methods

The impact of cardiovascular magnetic resonance image-derived markers extracted by machine learning algorithms was compared to the future risk of adverse events in a group of 44,957 UK Biobank participants.

Results

Most markers, including the left ventricular ejection fraction, have limited prognostic value. GLASED was significantly associated with all-cause mortality and major adverse cardiovascular events, with the largest hazard ratio, highest ranking and differentiated risk in all three tertiles ($P \leq 0.0003$).

Conclusions

GLASED predicted all-cause mortality and major cardiovascular adverse events better than conventional markers of risk and is recommended for assessing patient prognosis.

Title Page

Global Longitudinal Active Strain Energy Density (GLASED): A Powerful Prognostic Marker in a Community-Based Cohort

Authors:

Nay Aung^{1,2} MBBS MRCP PhD, David H. MacIver^{3,4} MBBS MD T(M) FRCP EFESC, Henggui Zhang³ PhD FRSA FRSB, Sucharitha Chadalavada^{1,2} MBBS MRCP and Steffen E. Petersen^{1,2} MSc MPH MD DPHIL SFHEA FRCP FSCMR FJCS FACC FEACVI FESC.

Institutions:

- 1) William Harvey Research Institute, NIHR Barts Biomedical Research Centre, Queen Mary University London, Charterhouse Square, London, EC1M 6BQ, UK
- 2) Barts Heart Centre, St Bartholomew's Hospital, Barts Health NHS Trust, West Smithfield, EC1A 7BE, London, UK
- 3) Biological Physics Group, Department of Astronomy and Physics, University of Manchester, Manchester, United Kingdom.
- 4) Department of Cardiology, Taunton & Somerset Hospital, United Kingdom.

Short title: GLASED: A powerful prognostic marker

Correspondence: Professor David H MacIver, MB BS, MD, T(M), FRCP, EFESC. Biological Physics Group, Department of Astronomy and Physics, University of Manchester, Manchester, United Kingdom. david.maciver@manchester.ac.uk

Contributions:

SC derived the strain measurements. NA performed the extraction of all other image-derived markers and statistical analyses. DHM conceived the project and wrote the first draft. HZ provided essential engineering and physics expertise. SEP had a supervisory role, helped with the study design and performed major manuscript edits. All the authors contributed, provided critical feedback, agreed to the manuscript and have equal responsibility for its content.

Data availability request:

This research was conducted using the UK Biobank resource under access application 2964. The UK Biobank will make the data available to all bona fide researchers for all types of health-related research that is in the public interest, without preferential or exclusive access for any persons. All researchers will be subject to the same application process and approval criteria as specified by the UK Biobank. For more details on the access procedure, see the UK Biobank website: <http://www.ukbiobank.ac.uk/register-apply/>.

Other information, including a prewritten Excel template for calculating GLASE and GLASED, is available from the corresponding author upon reasonable request.

Index terms/Key words

contractance, contractility, contractile function, energy, heart failure, systolic function, stroke work

Abbreviations:

AIC, Akaike information criterion

BMI, body mass index

BSA, body surface area

CMR, cardiac magnetic resonance imaging

GLASE, global longitudinal active strain energy

GLASED, global longitudinal active strain energy density

GLS, absolute peak global longitudinal strain

HR, hazard ratio

LV, left ventricle/ventricular

LVCF, left ventricular contraction fraction

LVEF, left ventricular ejection fraction

LVGFI, left ventricular global function index

LVMV, left ventricular muscle volume

MACE, major adverse cardiovascular event(s)

Conflict of interest statement:

SEP - Consultancy, Circle Cardiovascular Imaging Inc., Calgary, Alberta, Canada.

Ethical approval

Overall ethical approval for UK Biobank studies was obtained from the NHS National Research Ethics Service on 17th June 2011 (Ref 11/NW/0382); this approval was extended on 18 June 2021 (Ref 21/NW/0157).

Acknowledgements

This study was conducted using the UK Biobank resource under access application 2964.

We would like to thank all the participants and staff involved in planning, collection and analysis, including core laboratory analysis of the CMR imaging data.

Linkage Data Acknowledgements

Please refer to the following guidance from NHS Digital and Public Health Scotland regarding the acknowledgement of data linkage.

NHS Digital

Researchers using data from NHS Digital must cite the copyright of NHS Digital as follows: "Copyright © (year), NHS Digital. Re-used with the permission of the NHS Digital [and/or UK Biobank]. All rights reserved." Where practicable, outputs cite the source of the data as "this work uses data provided by patients and collected by the NHS as part of their care and support."

Public Health Scotland

Attribution Statement - Please acknowledge National Safe Haven for providing access to the data assets and the environment, which was made available as part of the Data and Connectivity National Core Study Programme in papers and other research outputs. For example, this research used data assets made available by National Safe Haven as part of the Data and Connectivity National Core Study, led by Health Data Research UK in partnership with the Office for National Statistics and funded by UK Research and Innovation (research that commenced between 1st October 2020 and

31st March 2021 grant ref MC_PC_20029; 1st April 2021 and 30th September 2022 grant ref MC_PC_20058).

Word count:

Main manuscript: Abstract 170 words, Main manuscript 5,320 words including references. Tables and legends 686 words. References 30

Funding section/Disclosures:

Barts Charity (G-002346) contributed to the fees required to access the UK Biobank data [access application #2964]. SEP acknowledges the British Heart Foundation for funding the manual analysis to create a cardiovascular magnetic resonance imaging reference standard for the UK Biobank imaging resource in 5000 CMR scans (www.bhf.org.uk; PG/14/89/31194).

NA acknowledges support from the Medical Research Council for his Clinician Scientist Fellowship (MR/X020924/1).

SEP acknowledges support from the National Institute for Health and Care Research (NIHR) Biomedical Research Centre at Barts.

SEP and SC have received funding from the European Union's Horizon 2020 Research and Innovation Programme under grant agreement No. 825903 (euCanSHare project).

SEP acknowledges support from the "SmartHeart" EPSRC programme grant (www.nihr.ac.uk; EP/P001009/1) and consultancy with Circle Cardiovascular Imaging, Inc., Calgary, Alberta, Canada

This article is supported by the London Medical Imaging and Artificial Intelligence Centre for Value Based Healthcare (AI4VBH), which is funded by the Data to Early Diagnosis and Precision Medicine strand of the government's Industrial Strategy Challenge Fund and managed and delivered by the Innovate UK on behalf of UK Research and Innovation (UKRI). The views expressed are those of the authors and not necessarily those of the AI4VBH Consortium members, the NHS, the Innovate UK, or the UKRI.

The funders provided support in the form of salaries for the authors as detailed above but did not have any additional role in the study design, data collection and analysis, decision to publish, or preparation of the manuscript.

Introduction

Determining the optimal predictive imaging markers in patients with left ventricular heart disease is crucial for guiding management decisions. However, the most reliable measures of left ventricular (LV) structure or function for determining future risk are unclear.

In this study, we compared the predictive performance of the recognised measures of LV structure and function, with a particular focus on a new method called global longitudinal active strain energy density (GLASED).¹

At least 23 LV imaging markers, including left ventricular ejection fraction (LVEF),² end-diastolic volume,³ left ventricular mass,⁴ myocardial strain,⁵ strain rate,⁶ pressure-strain product,⁷ stroke work, stroke work indexed to left ventricular mass,¹ global function index,⁸ contraction fraction⁹ and GLASED, have been advocated for the assessment of contractile function and/or risk.¹ However, to date, a comprehensive assessment of the relative effectiveness of these potential risk markers has not been undertaken.

Although the LVEF is widely used for risk assessment, it has serious limitations in predicting the prognosis of patients with HF syndromes.^{2, 10-12} While myocardial strain has some prognostic value,^{6, 13} it is limited by its inability to consider afterload.⁵ A greater afterload results in reduced myocardial shortening.^{14, 15} Therefore, afterload not only impacts strain interpretation but also indirectly affects LVEF because LVEF itself is influenced by strain.¹⁶ An accurate method to correct myocardial shortening during afterload has been sought for more than two decades.¹⁵

Contractance is a new measure of contractile function derived from the area under a stress-strain curve¹⁴ and can be estimated in whole ventricles using GLASED.¹ GLASED overcomes the limitations of other methods, including strain, by accurately allowing for the effect of afterload, including remodelling. GLASED estimates the mechanical energy (work done) per unit volume of myocardium during contraction. As such, it is likely to be a more robust measure of myocardial contractile function than alternative measures. Blood pressure, wall thickness, chamber dimensions (determinants of wall stress) and myocardial strain are required for its calculation. GLASED confers a robust theoretical advantage over other approaches for evaluating left ventricular systolic function because strain energy density has a strong background in engineering science. Furthermore, a recent study of a large cohort of patients referred for cardiac magnetic resonance imaging (CMR) showed that GLASED is the best predictor of expected prognosis and BNP compared with LVEF, stroke work, stroke work per LV mass, pressure-strain product, LV contraction fraction (LVCF), and strain.¹

Moreover, according to echocardiographic analyses, the GLASED was significantly lower in veteran athletes than in young athletes and greater in young male athletes than in young female athletes.¹⁷

Global longitudinal active strain energy (GLASE), calculated by multiplying GLASED with the left ventricular muscle volume (LVMV), is a measure of the total work performed by the left ventricular muscle in the longitudinal direction. GLASE provides similar information to stroke work but is derived from information obtained from the myocardium rather than from the lumen. Therefore, GLASE accounts for myocardial shortening, geometric differences (wall thickness and internal dimensions), systolic blood pressure and muscle volume, whereas stroke work accounts for only systolic pressure and stroke volume. While GLASED measures the myocardium's health or (dys)function, GLASE indicates whether there is sufficient myocardium (adequate hypertrophy) to generate the energy necessary for a normal left ventricular output that meets the needs of the body.

Given the theoretical benefits of GLASED, combined with the recent prognostic CMR study,¹ our principal a priori hypothesis was that GLASED would be a superior predictor of outcome compared with more conventional markers. Therefore, we aimed to evaluate the impact of various measures of LV structure and contractile function on all-cause mortality (primary endpoint) with MACE and heart failure risk (secondary endpoints) in a community-based longitudinal cohort study using the UK Biobank database.

Methods

Study cohort

The UK Biobank is a prospectively recruited population study of more than 500,000 volunteers living in the United Kingdom that provides information on demographics, lifestyle, medical background, physical measurements, genomics and proteomics.¹⁸ The UK Biobank population cohort was 40-69 years of age and was initially recruited between 2006 and 2010. The enrichment of the original cohort with imaging data, including CMR data, commenced in 2014. The UK Biobank aimed to recruit a cohort that is representative of the UK population sample. Consequently, the investigators did not seek healthy volunteers or oversample people with any health conditions. Ethical approval for the UK Biobank studies was obtained from the NHS National Research Ethics Service on 17th June 2011 (Ref 11/NW/0382); this approval was extended on 18th June 2021 (Ref 21/NW/0157).

Imaging analysis

In-depth information on the UK Biobank CMR imaging protocol commencing in 2014 is available elsewhere.¹⁹ In total, CMR images from 44,957 individuals were available at the time of this study. Segmentation and derivation of other LV markers were performed using a fully convolutional neural

network trained on expert-annotated data from the first 4,875 CMR studies as previously described^{20, 21}. We excluded individuals with inadequate quality imaging data detailed in prior publications.^{22, 23}

Left ventricular assessment

Peak global longitudinal myocardial strain (GLS) was measured using a feature-tracking algorithm implemented in CVI42 software (Circle, prototype v5.13.7). GLS was calculated using all three long-axis images, i.e., 3-chamber, 2-chamber and 4-chamber views. Endo- and epicardial contours (excluding extreme basal slices that included the left ventricular outflow tract) were drawn using automated algorithms. Feature tracking markers were attached to the whole myocardium within the defined epicardial and endocardial borders and tracked throughout the cardiac cycle with end diastole as the reference phase. The calculation was made from the longitudinal change detected by multiple trackers of the myocardium to produce the peak GLS using the Green–Lagrange strain method. The LV muscle volume (LVMV) was measured using rounded contours at the blood/myocardial border and excluded papillary muscles and trabeculations. The LV mass was calculated from the LVMV multiplied by the density of myocardial tissue (1.05 g/ml). LV mass was indexed to body surface area (BSA) and height^{2.7} (height in meters to a power of 2.7).

The left ventricular global function index (LVGFI) was calculated from the following equation:⁸

$$LVGFI = SV / [LVMV + (ESV + EDV)/2]$$

where *SV* is the stroke volume, *ESV* is the end-systolic volume and *EDV* is the end-diastolic volume.

The LV (myocardial) contraction fraction (LVCF) was calculated as follows⁹:

$$LVCF = SV/LVMV$$

Stroke work was estimated from the product of stroke volume and systolic blood pressure.¹ Stroke work was indexed to the BSA and height^{2.7}.

The pressure-strain product (%mmHg) was calculated as the product of the absolute strain (%) and the systolic BP (mmHg).⁷

The Lamé equation for longitudinal stress is more accurate than other methods and matches the results of left ventricular finite element analysis.²⁴ The peak nominal Lamé longitudinal stress (σ_1) was calculated using the following equation:^{1, 24}

$$\sigma_1 = \frac{P_i r_i^2}{(r_o^2 - r_i^2)}$$

where P_i is the inner pressure (in Pa) and is equal to the peak systolic pressure measured using a brachial cuff. Furthermore, r_o is the outer (epicardial) radius, and r_i is the inner (luminal or endocardial) LV radius at end-diastole. The inner luminal diameter was calculated as an average value of the measurements from the left ventricular endocardial contours of the basal to mid short-axis slices. The end-diastolic maximum wall thickness, which is required to estimate the outer (epicardial) radius, was calculated by taking the mean value of the wall thickness measurements in the American Heart Association (AHA) segments of the same basal to mid short-axis slices. The nominal (i.e., based on the pre-deformed configuration), rather than the instantaneous, stress was used because it correlates well with the numerical calculation (i.e., contractance).^{1,17}

GLASED was calculated using the following equation:¹

$$GLASED = \frac{1}{2} \times |\sigma_l| \times |\epsilon_l| \text{ (i.e., } \frac{1}{2} \times \text{longitudinal stress} \times \text{peak GLS)}$$

where $|\epsilon_l|$ and $|\sigma_l|$ are the absolute value (magnitude) of the nominal stress and peak global longitudinal strain (GLS) derived by tissue tracking, respectively, to give a positive value for the GLASED.

GLASE was calculated using the following equation:¹

$$GLASE = GLASED \times LVMV$$

GLASE was indexed to both BSA and height^{2,7}.

Prognosis

The primary endpoint was all-cause mortality, and the secondary endpoints were major adverse cardiovascular events (MACEs) and heart failure. Longitudinal follow-up was performed via linkage to Hospital Episodes Statistics (HES) data encoded in the International Classification of Disease 10th Revision (ICD10) classification system and national death registries. The ICD10 codes used to define MACE (which includes nonfatal or fatal myocardial infarction and stroke) and heart failure are detailed in Table S1.

Statistical analysis

The full details of the statistical analyses can be found in the Supplementary data. In brief, 4 main analyses were performed: 1. Cox proportional hazard ratios adjusted for age and sex (Model 1) and age and sex with all cardiovascular risk factors (Model 2); 2. The Akaike information criterion (AIC) was used to rank the predictive accuracy of the markers in Models 1 and 2. Kaplan-Meier survival analysis showing the unadjusted associations between LV markers and outcomes; 4) C-statistics. A

further subgroup analysis was performed on individuals with an LVEF > 55%. A Holm–Bonferroni-corrected *P* value of less than 0.05 was considered to indicate statistical significance.

Results

Demographics

The baseline characteristics of the study population are presented in Supplementary Table S2A. Our cohort consisted of 21,631 males and 23,326 females, and the overall mean age (SD) was 64 (8) years. The mean, standard deviation (SD), median, minimum and maximum values for the LV markers are also shown (Table S2A), and their distributions are shown in Figure S1. The participant characteristics stratified by cardiovascular disease (CVD) status are presented in Table S2B. The maximum follow-up duration was 6.8 years.

Relationships between LV markers and age, sex and risk factors

Age was associated with a smaller LV end-diastolic diameter and lower volume, LVCF, LVGFI, absolute GLS and GLASED (Figure S2). With increasing age, a higher wall stress, pressure-strain product and stroke work were observed.

LV mass, the end-diastolic diameter and volume were lower in females than in males. The left ventricular ejection fraction (LVEF), LVGFI, LVCF, and absolute GLS and GLASED were significantly greater in females than in males ($P < 0.0001$). The presence of the cardiovascular risk factors smoking, alcohol consumption, hypertension, diabetes mellitus and hyperlipidaemia were consistently associated with poorer LV functional markers, such as LVEF, LVCF, LVGFI, absolute GLS and GLASED.

A higher physical activity score was associated with a lower LVEF and greater LV dimensions, volumes, mass, LVCF, absolute GLS and GLASED, but there was no difference in the LVGFI (Figure S2).

Prognostic association with all-cause mortality

After a median (interquartile range [IQR]) follow-up of 2.7 (1.9 to 4.1) years, 413 (0.9%) participants died. Higher LV mass (indexed and non-indexed) or lower LVEF, LVCF, LVGFI, absolute GLS and GLASED were associated with a greater incidence of death in both models (Table S3A). GLASED had the largest magnitude of effect size (HR 1.38, CI: 1.13 to 1.68, $P = 0.001$) in predicting death in comparison to the next strongest marker, GLS (HR = 1.09, 95% CI: 1.04 to 1.15, $P = 0.0007$) (Tables S3A, S4 and Figure 1A, Model 1). Only modest effect sizes were detected for the other LV markers (the mean HR ranged from 1.01 to 1.09 per SD change). LV cavity size, wall stress, pressure-strain product, stroke work, stroke work indexed to the BSA, stroke work indexed to height^{2.7}, GLASE, GLASE indexed to BSA and GLASE indexed to height^{2.7} did not predict all-cause mortality.

Prognostic associations with major adverse cardiovascular events

In our study population, 831 (1.8%) individuals experienced MACE over a median follow-up of 2.7 years. Greater LV mass and lower LVEF, LVCF, LVGFI, absolute GLS and GLASED were consistently associated with a greater risk of incident MACE across both models (Figure 1B and Table S3B). In Model 1, GLASED had the highest HR (1.39, CI: 1.21 to 1.61, $P < 0.0001$), followed by GLS (HR = 1.12, 95% CI: 1.08 to 1.16, $P < 0.0001$).

Prognostic associations with heart failure

A total of 245 (0.5%) participants were hospitalised with HF after a median follow-up of 2.7 years. A greater LV end-diastolic diameter and volume, greater unindexed and indexed LV mass, and lower absolute GLS and GLASED were associated with a greater risk of incident HF in a Cox model adjusted for age and sex (Figure 1C, Model 1). A lower LVEF, LVCF, LVGFI and stroke work indexed to LV mass were associated with a greater risk of heart failure (Table S3C). For HF risk, the LV end-diastolic diameter indexed to height^{2.7} had the largest effect size (HR = 1.45, 95% confidence interval [CI]: 1.33 to 1.57, $P < 0.0001$), followed by GLASED (HR = 1.41, 95% CI: 1.06 to 1.88, $P = 0.019$) and GLS (HR = 1.30, 95% CI: 1.21 to 1.40, $P < 0.0001$).

Additional adjustment for conventional cardiovascular risk factors (Model 2) rendered the prognostic association between GLASED and heart failure non-significant. The other associated LV markers from Model 1 had slightly attenuated effect sizes while retaining statistical significance in Model 2 (Figure 1C and Table S3C). Table S4 shows the comparison of HR between GLASED and the other potential prognostic markers for heart failure, MACE and all-cause mortality.

Prognostic associations in the normal LVEF subgroup

After subgroup analysis of individuals with a normal LVEF (defined as $>55\%$), GLASED remained a strong predictor of MACE and all-cause mortality, with a greater HR than GLS (Model 1, HR = 1.39; CI: 1.18 to 1.64; $P < 0.0001$ vs HR = 1.13; CI: 1.08 to 1.18; $P < 0.0001$ for MACE and Model 1, HR = 1.38; CI: 1.11 to 1.73; $P = 0.005$ vs HR = 1.10; CI: 1.03 to 1.17; $P = 0.003$ for all-cause mortality); however, LVEF was not significantly associated with these outcomes (Tables S5A-S5C). Other LV markers were either not predictive or had a small effect size (mean HR range: 1.01 to 1.09) for MACE and all-cause mortality. For HF, LVEF and GLASED were not associated with incident events, but LV mass, LV end-diastolic volume and GLS remained significantly associated with incident events.

Akaike information criterion ranking

The model fit assessment demonstrated that GLASED had the best predictive performance for all-cause mortality according to the AIC compared to the other LV markers (Table 1). The GLASED ranking was followed by GLASE/BSA, GLASE/height^{2.7}, GLASE, the pressure-strain product, GLS and Lamé wall stress (Table 1). Notably, the C-statistics, which indicate the model's discriminative performance, of different LV markers were broadly comparable in the models for all-cause mortality (Tables S3A-S3C). There was no evidence of violation of the proportional hazard assumption in the Cox models on inspection of the Shoenfeld residuals. With MACE, GLASED had the best prediction model that fit the data best, followed by GLASE/height^{2.7}, GLASED/BSA, the pressure-strain product, GLS and the Lamé wall stress (Table 2). For heart failure, GLASE/height^{2.7}, GLASE/BSA, and GLASE, followed by GLASED, GLS, pressure strain product and Lamé longitudinal stress, performed best (Table 3).

Kaplan–Meier cumulative hazards of potential prognostic markers

The unadjusted Kaplan–Meier cumulative hazards for all-cause mortality for GLASED, GLS and LVEF are shown in Figure 2, and all-cause mortality, MACE and heart failure risk for all the markers are shown in Figures S4A-S4C. The lowest tertile of LVEF had the highest number of MACE ($P<0.0001$), heart failure ($P<0.0001$) and all-cause mortality ($P=0.001$), but there was no difference between the other two tertiles for any event.

Analysis of global longitudinal strain revealed differences in all 3 tertiles for MACE ($P=1\times 10^{-4}$) and all-cause mortality ($P=0.015$) but did not reveal differences in heart failure risk in two of the three tertiles (Figures 2 and S4). The lowest stress tertile was also linked to the highest risk of MACEs ($P<0.00001$) and all-cause mortality ($P=0.014$) but did not predict heart failure risk ($P=0.7$). The pressure-strain product did not predict the risk of either all-cause mortality or MACE; although heart failure risk was significant ($P=0.0075$), it did not differ between the upper two tertiles.

Stroke work was associated with a greater risk of MACEs in the highest tertile ($P=0.02$) but not with heart failure risk or all-cause mortality. Stroke work indexed to height^{2.7} or body surface area did not predict future risk. Stroke work indexed to LV mass showed that the risk of MACE ($P<0.0001$), heart failure risk ($P<0.0001$) and all-cause mortality ($P=0.001$) were greatest in the lowest tertile only ($P<0.001$) and did not distinguish between Q2 and Q3 for any outcome (Figure S4).

The hard endpoint of all-cause mortality (primary endpoint) was best identified by GLASED, with the lowest P value ($P=0.0003$) combined with good separation between tertiles (Figures 2 and S4).

According to post hoc analysis, the GLASED was significantly lower in individuals diagnosed with atrial fibrillation (Table S6).

Correlation of the potential prognostic markers

There were significant correlations between different LV markers (Figure S3). The strongest correlation was observed between the LV ejection fraction and the LVGFI ($r = 0.93$, $P < 0.0001$) and between GLASE/height^{2.7} and GLASE/BSA ($r = 0.93$, $P < 0.0001$). GLASED was strongly correlated with stroke work indexed to LV mass ($r = 0.8$); moderately correlated with GLS, LVCF and LVGFI ($r = 0.69$, 0.64 and 0.5 , respectively); and weakly correlated with LVEF ($r = 0.3$). The stress and strain were weakly correlated ($r = 0.24$, $P < 0.05$).

Discussion

To our knowledge, this is the first study to perform a comprehensive comparative analysis of potentially important prognostic markers of LV structure and contractile function in a large community-based cohort consisting of individuals with mostly normal LV structure (such as wall thickness and dimensions) and ejection fraction.

Sex differences

In accordance with the findings of previous studies,^{25, 26} we found a greater LVEF in females despite their lower wall thickness. Modelling suggested that this finding is a consequence of the lower end-diastolic diameter in females.^{17, 27} LV wall stress, the absolute GLS and the GLASED were greater in females. This result contrasts with our echocardiographic study in which young male athletes had a greater GLASED than female athletes.¹⁷ These sex differences were no longer present in the veteran athletes (mean age was 54 years). We speculate that the lower GLASED in males in this study reflects their greater age (mean 64 years) and corresponding greater incidence of CVD.

Predictor markers for all-cause mortality, MACEs and heart failure

An increase in LV mass slightly increased the risk of all outcomes, although an increase in LV mass indexed to height^{2.7} improved the prediction. The LVEF predicted heart failure risk to a modest extent but was a weak marker for assessing the risk of MACE or all-cause mortality. The unreliable nature of the LVEF stems from the effects of underlying variables that modulate it, such as changes in myocardial structure and strain.^{16, 27-30} A greater wall thickness or lower end-diastolic diameter increases the LVEF independently of myocardial strain.^{12, 16, 27-30} Global longitudinal strain performed better than LVEF in predicting the risk of heart failure, MACE and all-cause mortality. GLASED was the strongest marker for predicting the risk of MACEs and all-cause mortality (HR ≈ 1.4). The larger HR of

GLASED compared to that of GLS may reflect the impact of stress on the latter because GLASED corrects the GLS for afterload. The magnitude of the effect of GLASED for heart failure prediction was comparable to that of GLS (HR 1.41 vs 1.30). This finding may be a consequence of the inclination of clinicians to be more likely to diagnose heart failure in the presence of a dilated ventricle or reduced myocardial strain. GLASED is obtained by multiplying GLS by LV stress. In dilated ventricles, stress will increase, and thus, the GLASED will increase relative to the GLS. If dilated ventricles are overrepresented in the HF group, GLASED may be slightly overestimated, which would reduce its prediction power of HF.

There are theoretical reasons supporting the superiority of GLASED over other potential risk markers. GLASED inherently adjusts for both geometric changes and ventricular pressure. We posit that myocardial stress is a more accurate measure of afterload compared to BP alone. Cardiomyocytes primarily respond to LV stress rather than LV pressure, suggesting that the pressure-strain product might be less reliable than GLASED. The pressure-strain loop itself cannot directly quantify myocardial work; geometric data are essential for this purpose. Work is defined as force multiplied by distance, and work density is derived from the stress-strain loop, not the pressure-strain loop. Substituting luminal pressure for myocardial stress, as in the pressure-strain loop calculation, is inaccurate because: (a) luminal pressure exerts a force perpendicular to the stress experienced by the myocardium, and (b) it is stress, not luminal pressure, that is sensed by the cardiomyocytes. Pressure-strain loops serve as an indirect index of work and are only directly comparable when ventricular geometry remains constant. Consequently, the pressure-strain product/loop is expected to be less informative in cohorts exhibiting significant eccentric or concentric remodelling. In support of this, we have previously demonstrated that pressure-strain product was a less reliable predictor of mortality compared to GLASED in patient groups with substantial remodelling.¹ Similarly, the limited prognostic value of LVCF, LVGFI, and stroke work might be attributed to their inability to account for the influence of geometric changes due to dilation and wall thickness on stress.

A lower GLASED was associated with established cardiovascular risk factors such as smoking, diabetes, elevated BMI, hypertension, and hyperlipidaemia. This association arises because each of these factors independently affects both myocardial stress and strain. Since Model 2 incorporated these risk factors individually, the observed correlation between these factors and contractile stress/strain might explain the reduced predictive power of Model 2. This highlights the potential strength of the GLASED as a comprehensive marker that integrates the influence of conventional cardiovascular risk factors on clinical outcomes.

The left ventricular diastolic diameter indexed to height^{2,7} was strongly predictive of heart failure, which may indicate the presence of heart failure with a cause not primarily due to LV myocardial dysfunction, such as that due to left-sided valve regurgitation. Heart failure also occurs in patients with non-LV myocardial disorders, such as right heart failure, where the GLASED is expected to be normal. Furthermore, this finding should be treated with caution because the left ventricular diastolic diameter indexed to height^{2,7} was ranked last on the AIC (23rd) and was not significant according to the Kaplan–Meier curve ($P=0.62$). Furthermore, none of the other measures, such as the left ventricular diastolic diameter indexed to BSA or LV volume markers, performed well. The diagnosis of heart failure can be subjective, and factors such as myocardial strain and internal chamber dimensions obtained through imaging techniques can further influence diagnostic decisions. Heart failure risk may, therefore, represent a softer endpoint than MACE and all-cause mortality.

Limitations and Future Directions

Our cohort had a low pretest probability of events given their low rates of comorbidities and structural abnormalities. For example, in the UK Biobank cohort, only 2% of individuals had an LV wall thickness greater than 13 mm, which could have resulted in an underpowered assessment in this group. We found GLASED to be even more useful in predicting the expected prognosis in the presence of greater structural abnormalities such as amyloid heart disease and dilated cardiomyopathy.¹ Specifically designed prospective studies will be needed to assess the role of the GLASED and GLASE in predicting the risk of all adverse cardiovascular events.

GLASED is an approximation of myocardial longitudinal contractance derived using the area under the stress–strain curve¹⁴ but requires more sophisticated analyses that are currently unsuitable for clinical practice.¹ However, GLASED gives comparable results to those of an area under the curve method.^{1, 17} Future work should involve the automated calculation of GLASED, perhaps using machine learning algorithms with echocardiography, to allow widespread application.

The calculations of stress and the derived measurements of GLASED are prone to propagation error, emphasising that accurate measurements of wall thickness and end-diastolic diameter are important.

Ambulatory blood pressure data may improve the accuracy but were not available for this cohort. One advantage of our study is that it showed positive results with brachial blood pressure cuff measurements, so it is more easily applicable in clinical practice. No ‘diastolic function’ tests were performed, as this study principally aimed to assess geometry and systolic function, and the accuracy of diastolic function assessment using CMR is questionable. Strain rates were not assessed because

frame rates were too low for accurate results. Finally, information on major adverse cardiovascular events and heart failure was obtained from hospital admission records with potential encoding errors. For heart failure, we were unable to correlate our findings with more sensitive biomarkers, such as B-type natriuretic peptide (BNP), due to data unavailability.

While acknowledging the limitations of CMR for routine risk assessment in community settings, we propose that future investigations explore the potential of GLASED as a prognostic tool in broader patient populations. This could include cohorts with post-myocardial infarction, valvular disease, and hypertrophic cardiomyopathy, potentially using a more readily available modality like echocardiography.

Clinical perspective

Identifying the most powerful LV imaging marker(s) for assessing the outlook is crucial for understanding the pathophysiological mechanism of heart failure and exercise intolerance, guiding consensus documents, best patient management, and designing clinical intervention trials. GLASED overcomes the limitations of both GLS and LVEF by incorporating afterload correction and provides better prognostic information than current markers. The GLASED is applicable to both CMR and echocardiography¹⁷ and is easily and rapidly calculated from only 4 input variables.

GLASED offers a more direct assessment of myocardial function than prior methods. This advantage stems from its use of three key features: 1) direct myocardial data acquisition (rather than relying on luminal measurements), 2) estimation of energy production per unit of myocardial tissue, 3) incorporates left ventricular geometry and systolic pressure 4) integration of afterload correction of strain. Given these capabilities, GLASED has the potential to be valuable in evaluating the severity of LV myocardial dysfunction in various cardiac conditions, including valvular heart disease. A better risk stratification can be obtained by incorporating GLASED into cardiac imaging studies.

Conclusions

This exploratory analysis assessed the potential role of 23 different structural and functional prognostic markers of the left ventricle and compared them with a new measure of contractile function called the GLASED. GLASED is simple and quick to calculate from the mean wall thickness, end-diastolic diameter, systolic blood pressure and GLS. We showed that the left ventricular ejection fraction and multiple other potential left ventricular risk markers are of limited value in predicting patient prognosis. Despite our cohort consisting of low-risk individuals, GLASED improved the risk assessment of both major adverse cardiovascular events and all-cause mortality compared with other imaging measurements.

References

1. Maclver DH, Agger P, Rodrigues JCL, Zhang H. Left ventricular active strain energy density is a promising new measure of systolic function. *Sci Rep* 2022;**12**(1):1-14.
2. Bhatia RS, Tu JV, Lee DS, Austin PC, Fang J, Haouzi A, *et al.* Outcome of heart failure with preserved ejection fraction in a population-based study. *N Engl J Med* 2006;**355**(3):260-9.
3. White HD, Norris RM, Brown MA, Brandt PW, Whitlock RM, Wild CJ. Left ventricular end-systolic volume as the major determinant of survival after recovery from myocardial infarction. *Circulation* 1987;**76**(1):44-51.
4. Le TT, Lim V, Ibrahim R, Teo MT, Bryant J, Ang B, *et al.* The remodelling index risk stratifies patients with hypertensive left ventricular hypertrophy. *Eur Heart J Cardiovasc Imaging* 2021;**22**(6):670-679.
5. Smiseth OA, Aalen JM, Skulstad H. Heart failure and systolic function: time to leave diagnostics based on ejection fraction? *Eur Heart J* 2021;**42**(7):786-788.
6. Antoni ML, Mollema SA, Delgado V, Atary JZ, Borleffs CJ, Boersma E, *et al.* Prognostic importance of strain and strain rate after acute myocardial infarction. *Eur Heart J* 2010;**31**(13):1640-7.
7. Chan J, Edwards NFA, Khandheria BK, Shiino K, Sabapathy S, Anderson B, *et al.* A new approach to assess myocardial work by non-invasive left ventricular pressure-strain relations in hypertension and dilated cardiomyopathy. *Eur Heart J Cardiovasc Imaging* 2019;**20**(1):31-39.
8. Mewton N, Opdahl A, Choi EY, Almeida AL, Kawel N, Wu CO, *et al.* Left ventricular global function index by magnetic resonance imaging--a novel marker for assessment of cardiac performance for the prediction of cardiovascular events: the multi-ethnic study of atherosclerosis. *Hypertension* 2013;**61**(4):770-8.
9. Leibowitz D, Zwas D, Amir O, Gotsman I. The association between myocardial contraction fraction assessed by echocardiography and mortality. *Echocardiography* 2023;**40**(7):608-614.
10. Owan TE, Hodge DO, Herges RM, Jacobsen SJ, Roger VL, Redfield MM. Trends in prevalence and outcome of heart failure with preserved ejection fraction. *N Engl J Med* 2006;**355**(3):251-9.
11. Hogg K, Swedberg K, McMurray J. Heart failure with preserved left ventricular systolic function; epidemiology, clinical characteristics, and prognosis. *J Am Coll Cardiol* 2004;**43**(3):317-27.
12. Rodrigues JCL, Rooms B, Hyde K, Rohan S, Nightingale AK, Paton J, *et al.* The corrected left ventricular ejection fraction: a potential new measure of ventricular function. *Int J Cardiovasc Imaging* 2021;**37**(6):1987-1997.
13. Stanton T, Leano R, Marwick TH. Prediction of all-cause mortality from global longitudinal speckle strain: comparison with ejection fraction and wall motion scoring. *Circ Cardiovasc Imaging* 2009;**2**(5):356-64.
14. Maclver DH, Scrase T, Zhang H. Left ventricular contractance: A new measure of contractile function. *Int J Cardiol* 2023;**371**:345-353.
15. Schwitter J, De Marco T, Globits S, Sakuma H, Klinski C, Chatterjee K, *et al.* Influence of felodipine on left ventricular hypertrophy and systolic function in orthotopic heart transplant recipients: possible interaction with cyclosporine medication. *J Heart Lung Transplant* 1999;**18**(10):1003-13.
16. Maclver DH. The relative impact of circumferential and longitudinal shortening on left ventricular ejection fraction and stroke volume. *Exp Clin Cardiol* 2012;**17**(1):5-11.
17. Maclver DH, Zhang H, Johnson C, Papatheodorou E, Parry-Williams G, Sharma S, *et al.* Global Longitudinal Active Strain Energy Density (GLASED): Age and Sex Differences in young and Veteran Athletes. *MedRxiv* 2023;(also under review in **Echo Research & Practice**):2023.08.22.23294454.

18. Sudlow C, Gallacher J, Allen N, Beral V, Burton P, Danesh J, *et al.* UK biobank: an open access resource for identifying the causes of a wide range of complex diseases of middle and old age. *PLoS Med* 2015;**12**(3):e1001779.
19. Petersen SE, Matthews PM, Francis JM, Robson MD, Zemrak F, Boubertakh R, *et al.* UK Biobank's cardiovascular magnetic resonance protocol. *J Cardiovasc Magn Reson* 2016;**18**:8.
20. Bai W, Sinclair M, Tarroni G, Oktay O, Rajchl M, Vaillant G, *et al.* Automated cardiovascular magnetic resonance image analysis with fully convolutional networks. *J Cardiovasc Magn Reson* 2018;**20**(1):65.
21. Petersen SE, Aung N, Sanghvi MM, Zemrak F, Fung K, Paiva JM, *et al.* Reference ranges for cardiac structure and function using cardiovascular magnetic resonance (CMR) in Caucasians from the UK Biobank population cohort. *J Cardiovasc Magn Reson* 2017;**19**(1):18.
22. Aung N, Vargas JD, Yang C, Cabrera CP, Warren HR, Fung K, *et al.* Genome-Wide Analysis of Left Ventricular Image-Derived Phenotypes Identifies Fourteen Loci Associated With Cardiac Morphogenesis and Heart Failure Development. *Circulation* 2019;**140**(16):1318-1330.
23. Aung N, Lopes LR, van Duijvenboden S, Harper AR, Goel A, Grace C, *et al.* Genome-Wide Analysis of Left Ventricular Maximum Wall Thickness in the UK Biobank Cohort Reveals a Shared Genetic Background With Hypertrophic Cardiomyopathy. *Circ Genom Precis Med* 2023;**16**(1):e003716.
24. Maclver D, Zhang H. Quantifying myocardial active strain energy density: A comparative analysis of analytic and finite element methods for estimating left ventricular wall stress and strain. *Int J Cardiol* 2024 (in press <https://doi.org/10.1016/j.ijcard.2024.132139>).
25. Asch FM, Miyoshi T, Addetia K, Citro R, Daimon M, Desale S, *et al.* Similarities and Differences in Left Ventricular Size and Function among Races and Nationalities: Results of the World Alliance Societies of Echocardiography Normal Values Study. *J Am Soc Echocardiogr* 2019;**32**(11):1396-1406 e2.
26. Forsythe L, Maclver DH, Johnson C, George K, Somauroo J, Papadakis M, *et al.* The relationship between left ventricular structure and function in the elite rugby football league athlete as determined by conventional echocardiography and myocardial strain imaging. *Int J Cardiol* 2018;**261**:211-217.
27. Maclver DH. The impact of mitral regurgitation on left ventricular ejection fraction using mathematical modelling. *Exp Clin Cardiol* 2014;**20**(9):4994-5008.
28. Maclver DH, Townsend M. A novel mechanism of heart failure with normal ejection fraction. *Heart* 2008;**94**(4):446-9.
29. Maclver DH. A mathematical model of left ventricular contraction and its application in heart disease. In: Atherton M, Collins M, Dayer M, (eds). *Repair and Redesign of Physiological Systems*. Boston: WITpress; 2008, 65-86.
30. Rodrigues JC, Rohan S, Dastidar AG, Trickey A, Szantho G, Ratcliffe LE, *et al.* The Relationship Between Left Ventricular Wall Thickness, Myocardial Shortening, and Ejection Fraction in Hypertensive Heart Disease: Insights From Cardiac Magnetic Resonance Imaging. *J Clin Hypertens (Greenwich)* 2016;**18**(11):1119-1127.

Table 1. Model performance rankings for all-cause mortality events in fully adjusted Cox models (Model 2) by the Akaike information criterion (AIC), where lower values represent a better model fit

Rank	LV marker	AIC	Δ AIC
1	GLASED	6617.91	0.00
2	GLASE indexed to BSA	6622.05	4.14
3	GLASE indexed to height ^{2.7}	6622.11	4.20
4	GLASE	6622.38	4.46
5	Pressure-strain product	6733.41	115.50
6	Global longitudinal strain	6815.18	197.27
7	LV Lamé's wall stress	7030.60	412.68
8	Stroke work indexed to LV mass	7187.65	569.73
9	Stroke work indexed to height ^{2.7}	7194.94	577.02
10	Stroke work indexed to BSA	7195.09	577.17
11	Stroke work	7195.18	577.26
12	LV global functional index	7270.04	652.12
13	LV ejection fraction	7271.80	653.88
14	LV contraction fraction	7274.57	656.66
15	LV mass indexed to BSA	7275.81	657.90
16	LV mass indexed to height ^{2.7}	7276.51	658.60
17	LV mass	7276.96	659.04
18	LV end-diastolic volume indexed to BSA	7280.08	662.16
19	LV end-diastolic volume indexed to height ^{2.7}	7280.54	662.62
20	LV end-diastolic volume	7281.07	663.15
21	LV end-diastolic diameter indexed to BSA	7281.53	663.62
22	LV end-diastolic diameter	7281.79	663.88
23	LV end-diastolic diameter indexed to height ^{2.7}	7284.23	666.32

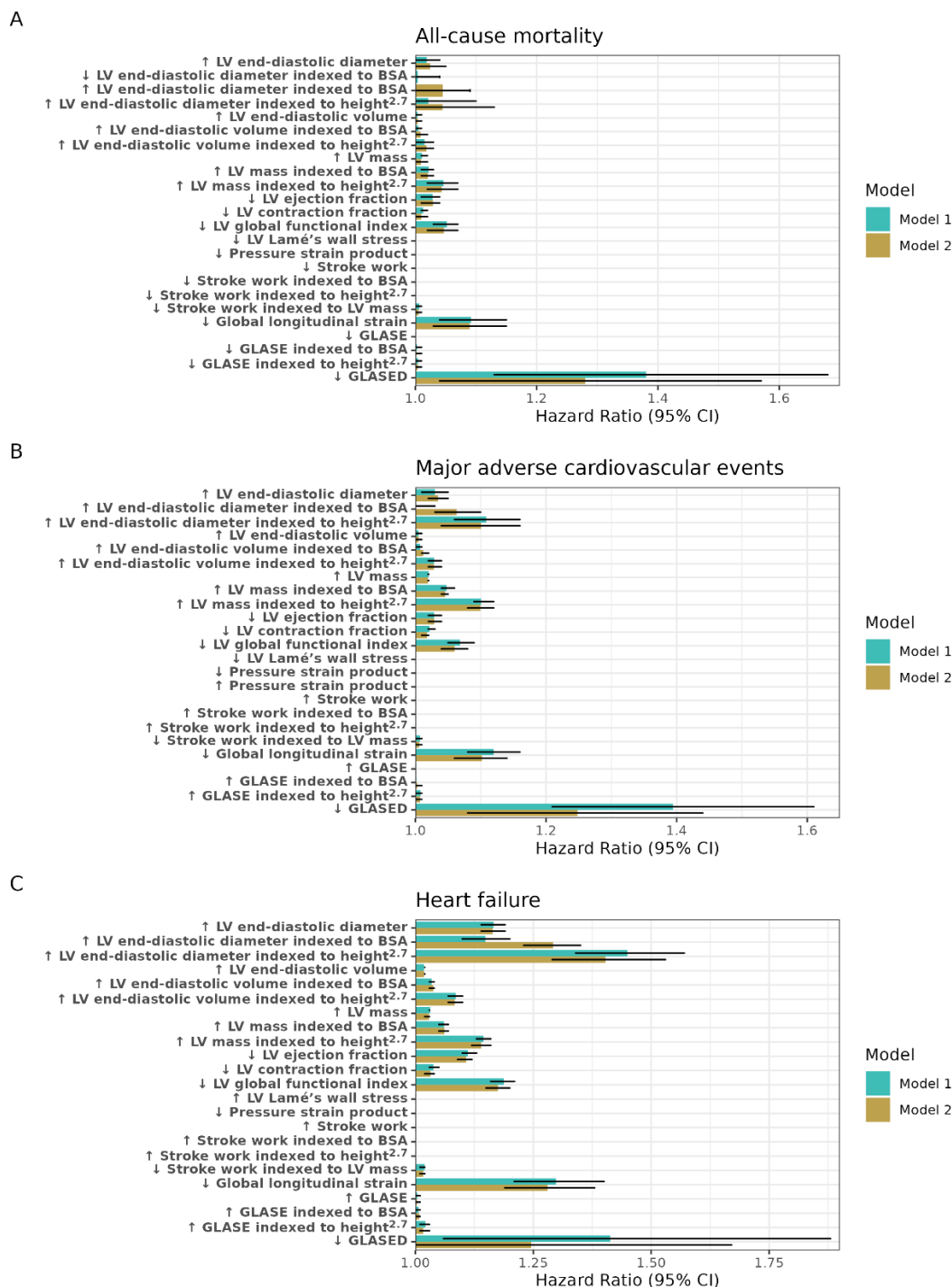
Table 2. Model performance rankings for major adverse cardiovascular events in fully adjusted Cox models (Model 2) by the Akaike information criterion (AIC), where lower values represent a better model fit

Rank	LV marker	AIC	Δ AIC
1	GLASED	13676.91	0.00
2	GLASE indexed to height ^{2.7}	13679.03	2.11
3	GLASE indexed to BSA	13679.61	2.70
4	GLASE	13680.00	3.08
5	Pressure-strain product	13988.92	312.01
6	Global longitudinal strain	14227.83	550.92
7	LV Lamé's wall stress	14683.49	1006.58
8	Stroke work indexed to LV mass	14955.13	1278.22
9	Stroke work indexed to height ^{2.7}	14964.86	1287.95
10	Stroke work indexed to BSA	14965.22	1288.30
11	Stroke work	14966.18	1289.27
12	LV mass indexed to BSA	15152.64	1475.73
13	LV mass indexed to height ^{2.7}	15155.30	1478.39
14	LV mass	15172.87	1495.96
15	LV contraction fraction	15192.90	1515.98
16	LV end-diastolic diameter	15212.99	1536.08
17	LV end-diastolic diameter indexed to BSA	15213.00	1536.09
18	LV global functional index	15213.15	1536.24
19	LV end-diastolic diameter indexed to height ^{2.7}	15215.50	1538.59
20	LV ejection fraction	15236.48	1559.57
21	LV end-diastolic volume indexed to height ^{2.7}	15238.68	1561.77
22	LV end-diastolic volume indexed to BSA	15241.71	1564.80
23	LV end-diastolic volume	15246.06	1569.14

Table 3 Model performance rankings for heart failure in fully adjusted Cox models (Model 2) by the Akaike information criterion (AIC), where lower values represent a better model fit

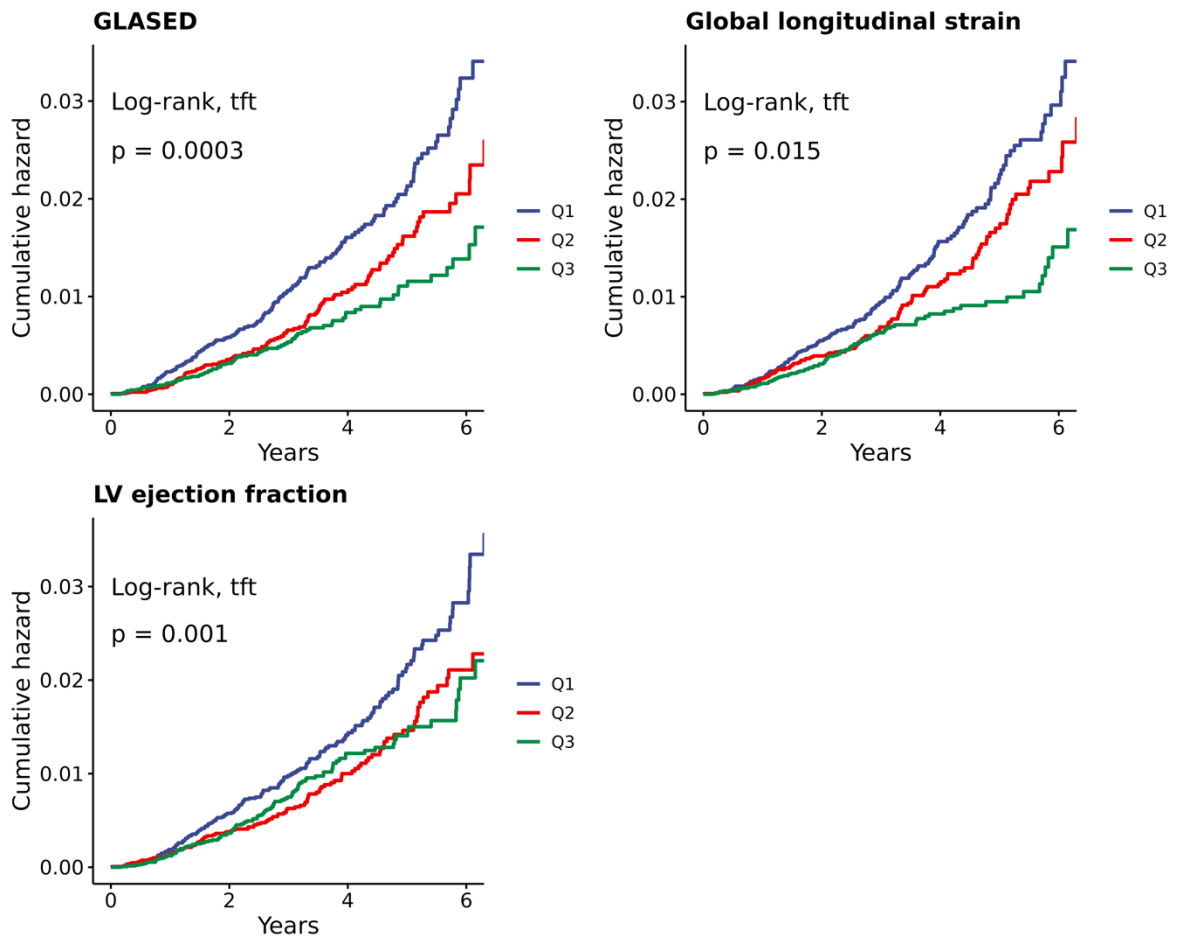
Rank	LV marker	AIC	Δ AIC
1	GLASE indexed to height ^{2.7}	3080.57	0.00
2	GLASE indexed to BSA	3080.61	0.03
3	GLASE	3081.51	0.94
4	GLASED	3087.01	6.44
5	Global longitudinal strain	3222.70	142.13
6	Pressure-strain product	3223.46	142.89
7	LV Lamé's wall stress	4078.12	997.55
8	LV ejection fraction	4177.55	1096.98
9	LV global functional index	4188.85	1108.28
10	LV end-diastolic diameter	4217.67	1137.09
11	Stroke work indexed to LV mass	4218.17	1137.60
12	LV end-diastolic volume indexed to BSA	4218.58	1138.01
13	LV end-diastolic volume	4226.51	1145.93
14	LV mass indexed to BSA	4226.83	1146.26
15	LV end-diastolic volume indexed to height ^{2.7}	4226.93	1146.36
16	LV mass indexed to height ^{2.7}	4232.60	1152.03
17	LV mass	4234.23	1153.66
18	LV end-diastolic diameter indexed to BSA	4237.61	1157.04
19	Stroke work	4263.24	1182.67
20	Stroke work indexed to BSA	4263.36	1182.79
21	Stroke work indexed to height ^{2.7}	4263.41	1182.84
22	LV contraction fraction	4268.40	1187.83
23	LV end-diastolic diameter indexed to height ^{2.7}	4282.04	1201.46

Figure 1. Cox proportional hazard ratios for potential prognostic markers corrected for age and sex (Model 1) and all risk factors (Model 2)



The hazard ratios and 95% confidence intervals represent the prognostic association of outcomes with one SD change (either increase or decrease, as indicated by the arrow) in LV markers. Model 1 was adjusted for age and sex, and Model 2 was adjusted for age, sex and cardiovascular risk factors (body mass index, hypertension, diabetes mellitus, dyslipidaemia, smoking history, regular alcohol intake, physical activity).

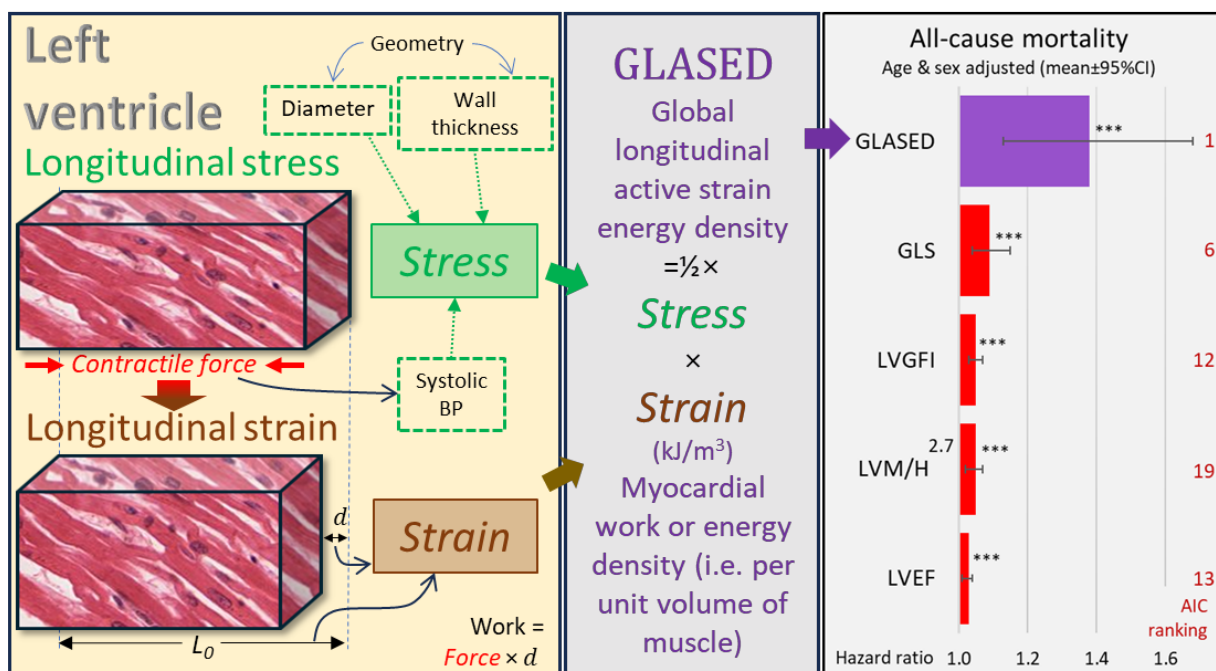
Figure 2. Kaplan-Meier cumulative hazards curves with potential prognostic markers in tertiles for all-cause mortality (see Figure S4 for all results)



Word count:

Main manuscript: Abstract 170 words, Main manuscript 5,320 words including references.
Tables and legends 686 words. References 30

Graphical abstract



1	Supplementary data
2	Index
3	Statistical analysis
4	Figures
5	Figure S1. Distribution of potential prognostic markers
6	Figure S2. Relationships between potential prognostic markers and age, sex and risk factors (by
7	univariate regression)
8	Figure S3A. Correlation matrix of potential prognostic markers (<i>r</i> values shown)
9	Figure S3B. <i>P</i> values for correlations of potential prognostic markers
10	Figure S4A. Kaplan-Meier cumulative hazards analysis with potential prognostic markers in tertiles for
11	all-cause mortality
12	Figure S4B. Kaplan-Meier cumulative hazards analysis with potential prognostic markers in tertiles for
13	major adverse cardiovascular events
14	Figure S4C. Kaplan-Meier cumulative hazards analysis with potential prognostic markers in tertiles for
15	heart failure risk
16	Tables
17	Table S1. The ICD10 codes used to define MACEs and heart failure
18	Table S2A. Demographics and main results (n=44,957)
19	Table S2B. Baseline characteristics stratified by cardiovascular disease status
20	Table S3A. Cox regression analysis of potential prognostic markers for all-cause mortality (Holm–
21	Bonferroni corrected $p < 0.05$ in bold)
22	Table S3B. Cox regression analysis of potential prognostic markers for major adverse cardiovascular
23	events (Holm–Bonferroni corrected $p < 0.05$ in bold)
24	Table S3C. Cox regression analysis of potential prognostic markers for heart failure (Holm–Bonferroni
25	corrected $p < 0.05$ in bold)
26	Table S4. Comparison of hazard ratios according to GLASED vs other potential prognostic markers
27	Table S5A. Cox regression analysis of potential prognostic markers for all-cause mortality in the
28	subgroup with a normal LVEF (>55%)
29	Table S5B. Cox regression analysis of potential prognostic markers for major adverse cardiovascular
30	events in the subgroup with a normal LVEF (>55%)
31	Table S5C. Cox regression analysis of potential prognostic markers for heart failure in the subgroup
32	with a normal LVEF (>55%)
33	Table S6. Atrial fibrillation and GLASED

34 **Statistical analysis**

35 Statistical analyses were performed using R version 4.1.1. Baseline characteristics are presented for
36 the whole cohort and were stratified by the presence or absence of CVD. Cardiovascular disease
37 status was ascertained from self-reported medical history taken at the time of the visit to the
38 imaging centre and included angina, heart attack/myocardial infarction, heart failure/pulmonary
39 oedema, arrhythmias, stroke, peripheral vascular disease, valvular heart disease, cardiomyopathy
40 and pericardial disease and prevalent MACE and heart failure identified from hospital episode
41 statistics (Table S1). Correlations between the potential prognostic markers were determined by
42 calculating the Pearson correlation coefficient (r). Univariate linear regression analysis was
43 performed to evaluate the associations between LV markers and age, sex, and conventional
44 cardiovascular risk factors. For GLS, we used absolute (positive) values for ease of interpretation.
45 Unadjusted associations between LV measurements stratified into tertiles and adverse outcomes
46 (heart failure incidence, MACE incidence and all-cause mortality) were examined via cumulative
47 hazard curves with the log-rank trend test to evaluate survival differences. We constructed Cox
48 proportional hazards models to examine the associations between LV markers and adverse outcomes
49 after accounting for potential confounders. In the primary analysis, the Cox model was adjusted for
50 age and sex (Model 1). A Holm–Bonferroni-corrected P value of less than 0.05 was considered to
51 indicate statistical significance in primary analyses. In the secondary sensitivity analyses, (i) we
52 adjusted for age and sex, cardiovascular risk factors (body mass index (BMI), smoking status, regular
53 alcohol intake, self-reported physical activity in total minutes per week, hypertension, diabetes
54 mellitus and hyperlipidaemia) (Model 2). (ii) We repeated Model 1 and Model 2 in a subset of
55 individuals with a normal LVEF ($>55\%$). Cardiovascular risk factors were ascertained from self-
56 reported medical history, secondary care records (HES data), the use of antihypertensive
57 medications, the use of lipid lowering medication or insulin, a total cholesterol concentration ≥ 7.0
58 mmol/L (to define hyperlipidaemia) and a glycated haemoglobin level (HBA1C) ≥ 48 mmol/mol (to
59 define diabetes mellitus). The level of physical activity was estimated with the International Physical
60 Activity Questionnaire.²⁶ Individuals who reported alcohol consumption three or more days per
61 week were classified as regular alcohol users. We centred and scaled the variables; therefore, the
62 effect sizes from the regression models represent the per standard deviation (SD) change in the
63 exposure variable. The proportional hazard assumption was assessed by checking the correlation of
64 Schoenfeld residuals with time. The differences in the hazard ratios (HRs) of the LV markers were
65 evaluated by an unpaired t test using the bootstrap resampling technique. The performance of
66 different LV markers in Cox models was compared by the Akaike information criterion (AIC), where
67 smaller values indicate a better model fit and greater predictive accuracy. The discriminative

68 performance of the LV markers was evaluated with Uno C-statistics, where larger values suggest
69 better performance.

70

Figure S1. Distribution of potential prognostic markers

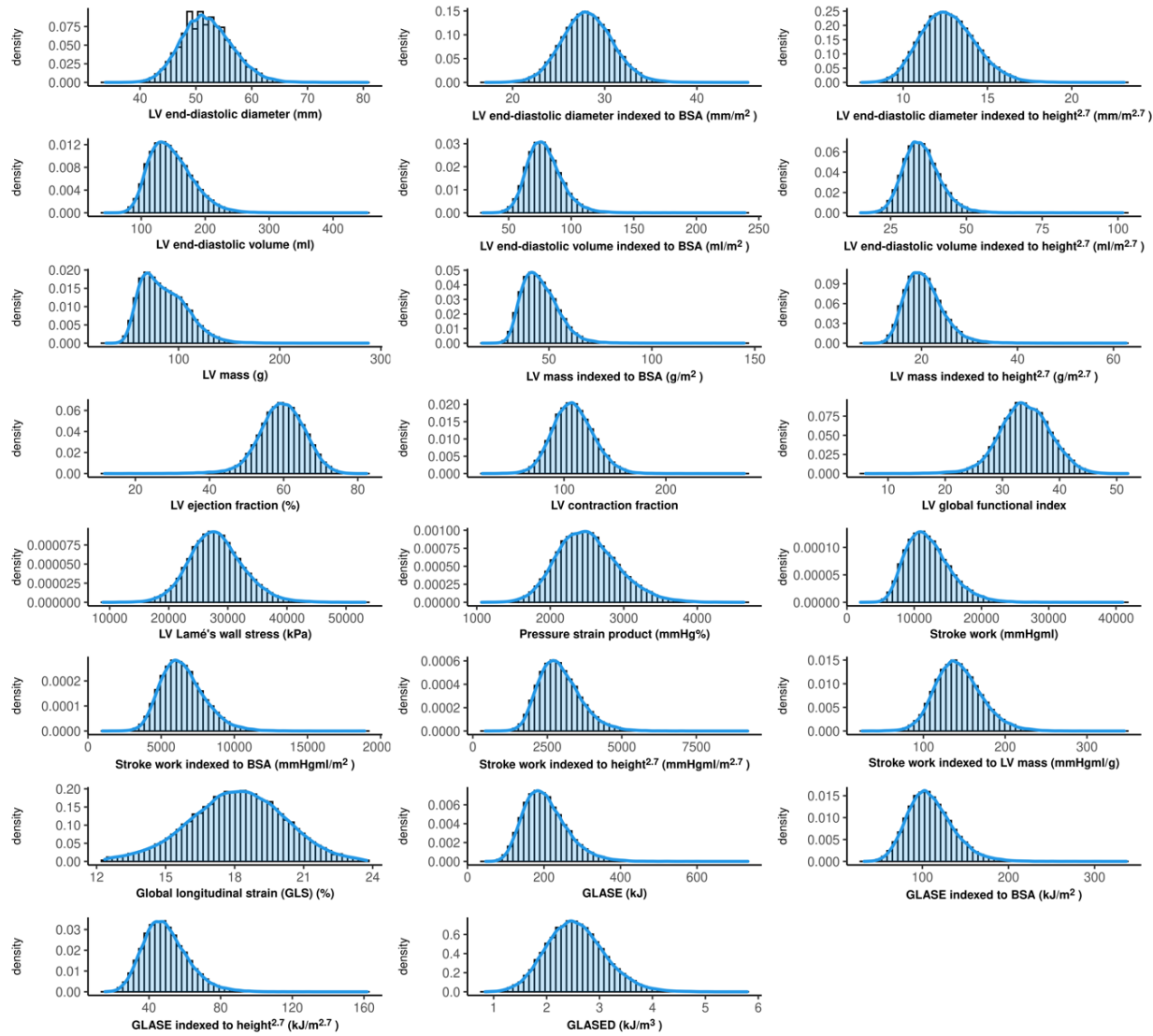


Figure S3A. Correlation matrix of potential prognostic markers (*r* values shown)

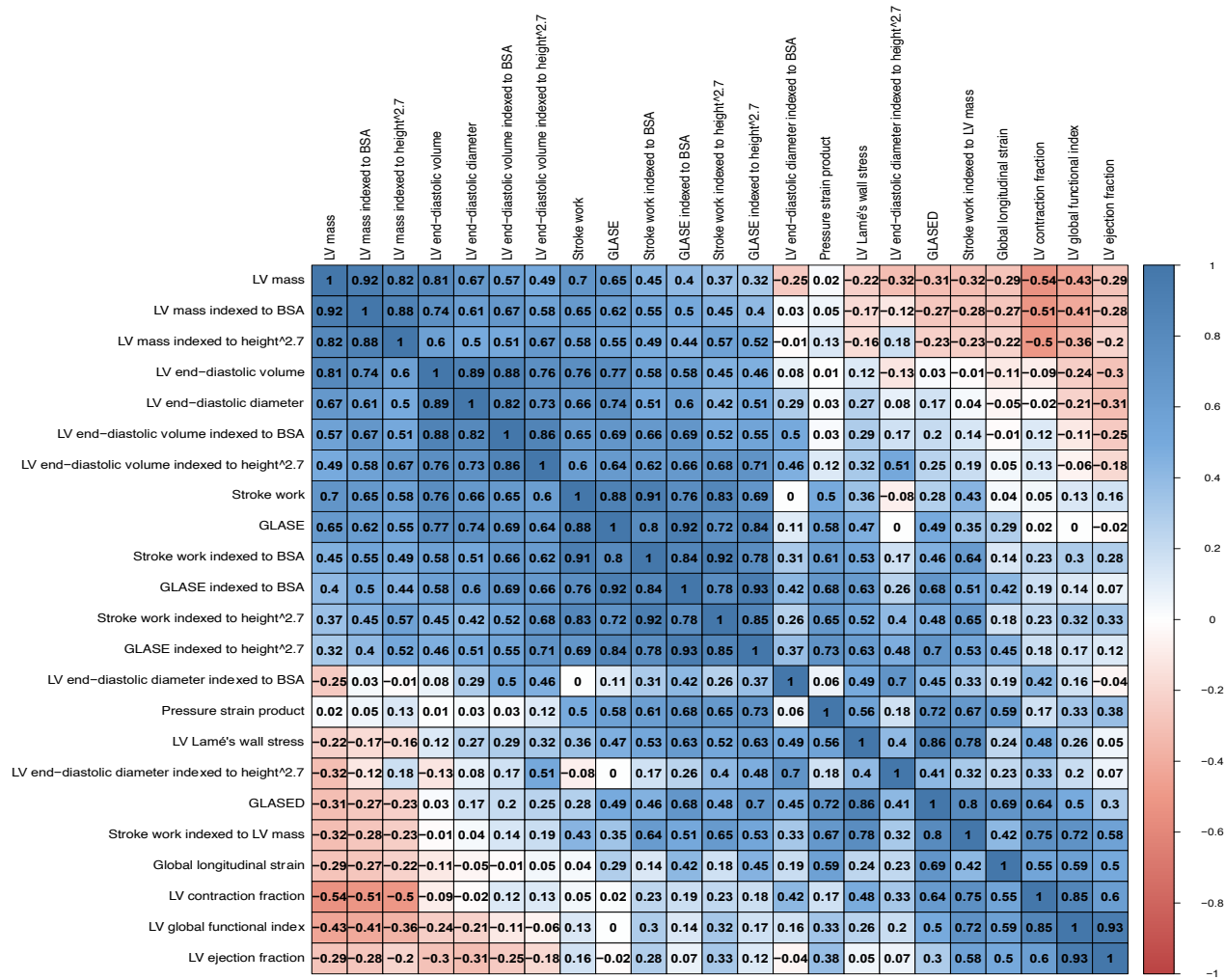


Figure S4A. Kaplan-Meier cumulative hazards analysis with potential prognostic markers in tertiles for all-cause mortality

All-cause mortality

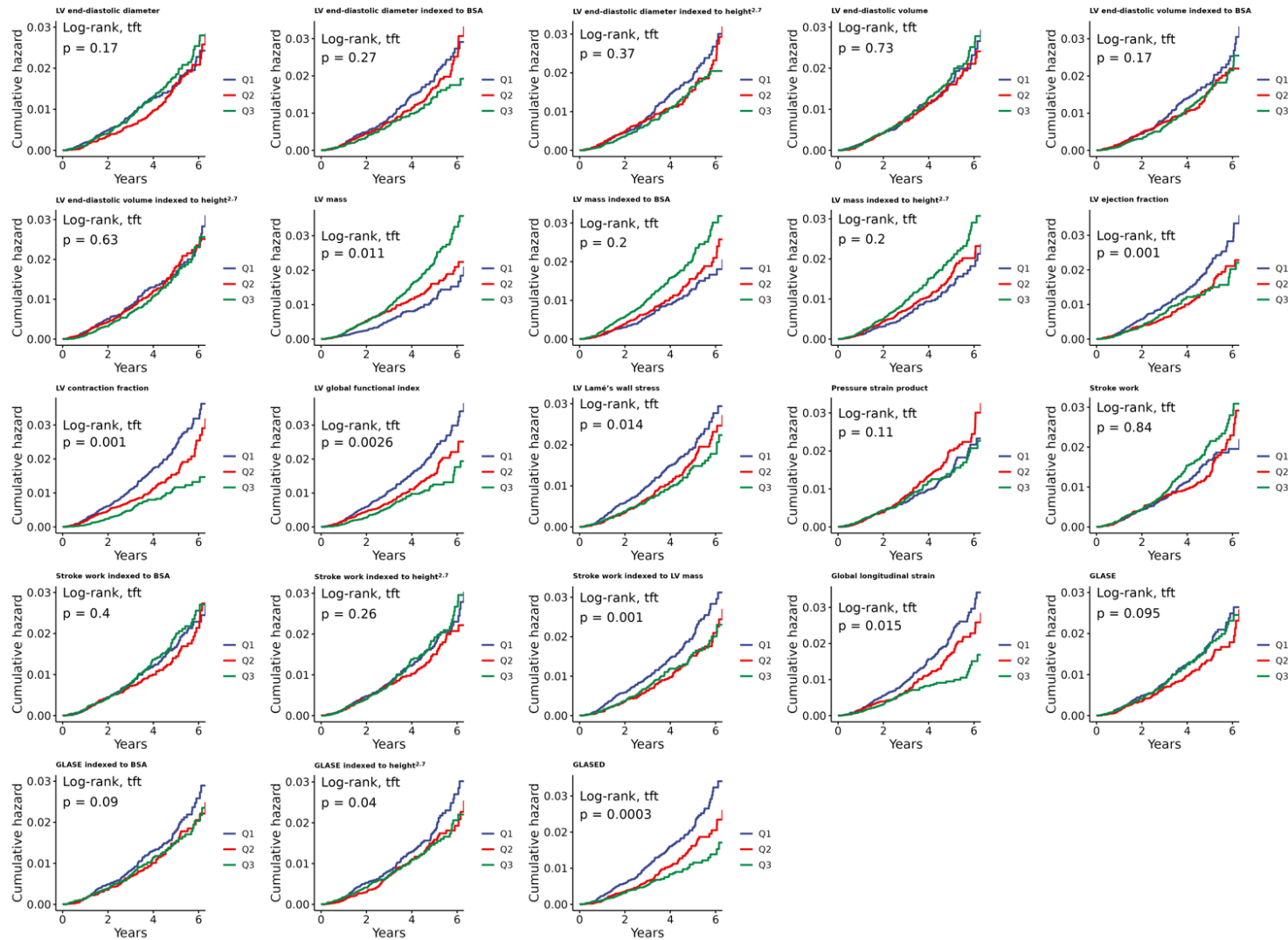


Figure S4B. Kaplan-Meier cumulative hazards analysis with potential prognostic markers in tertiles for major adverse cardiovascular events

Major adverse cardiovascular events

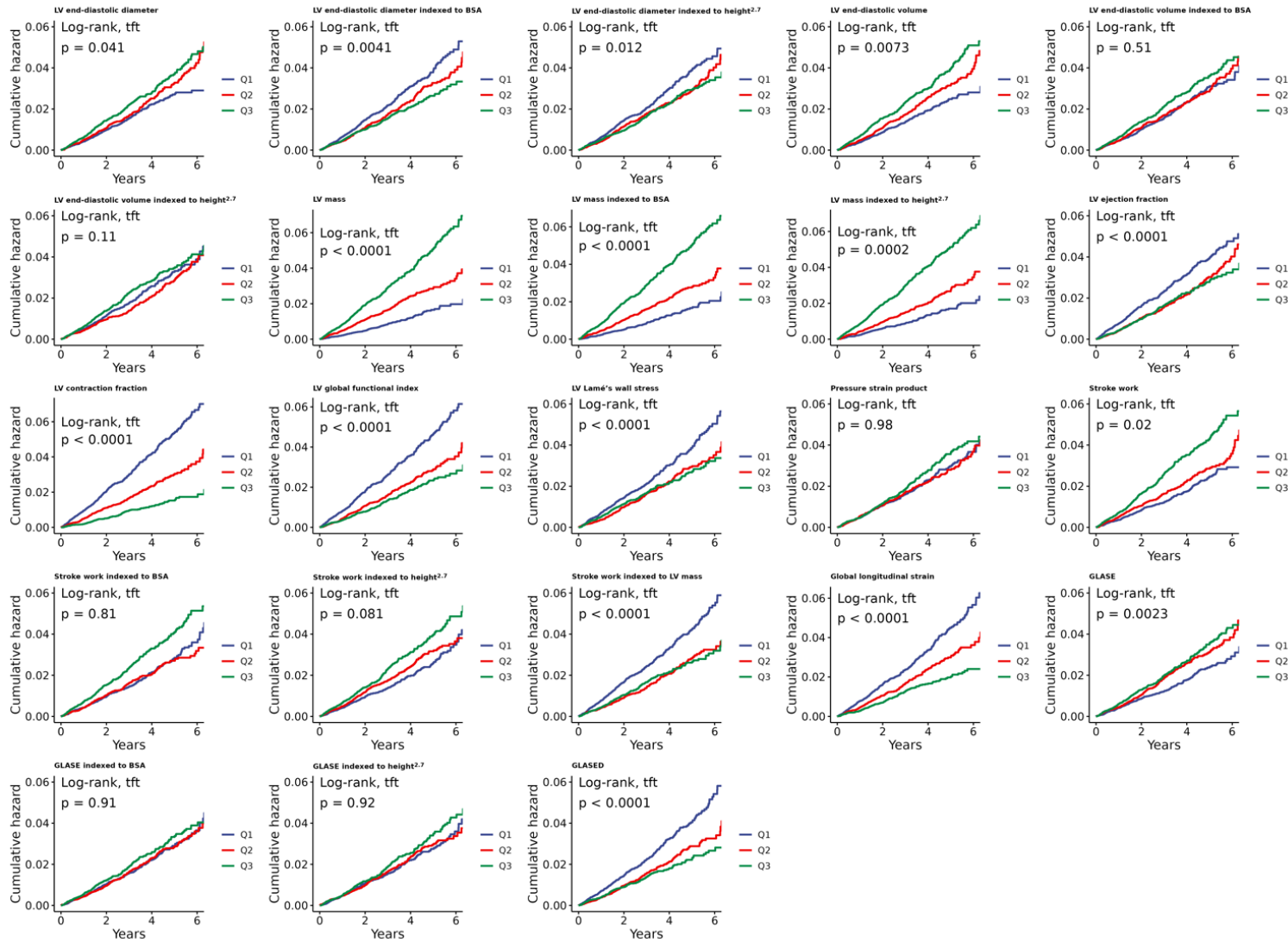


Figure S4C. Kaplan-Meier cumulative hazards analysis with potential prognostic markers in tertiles for heart failure risk

Heart failure

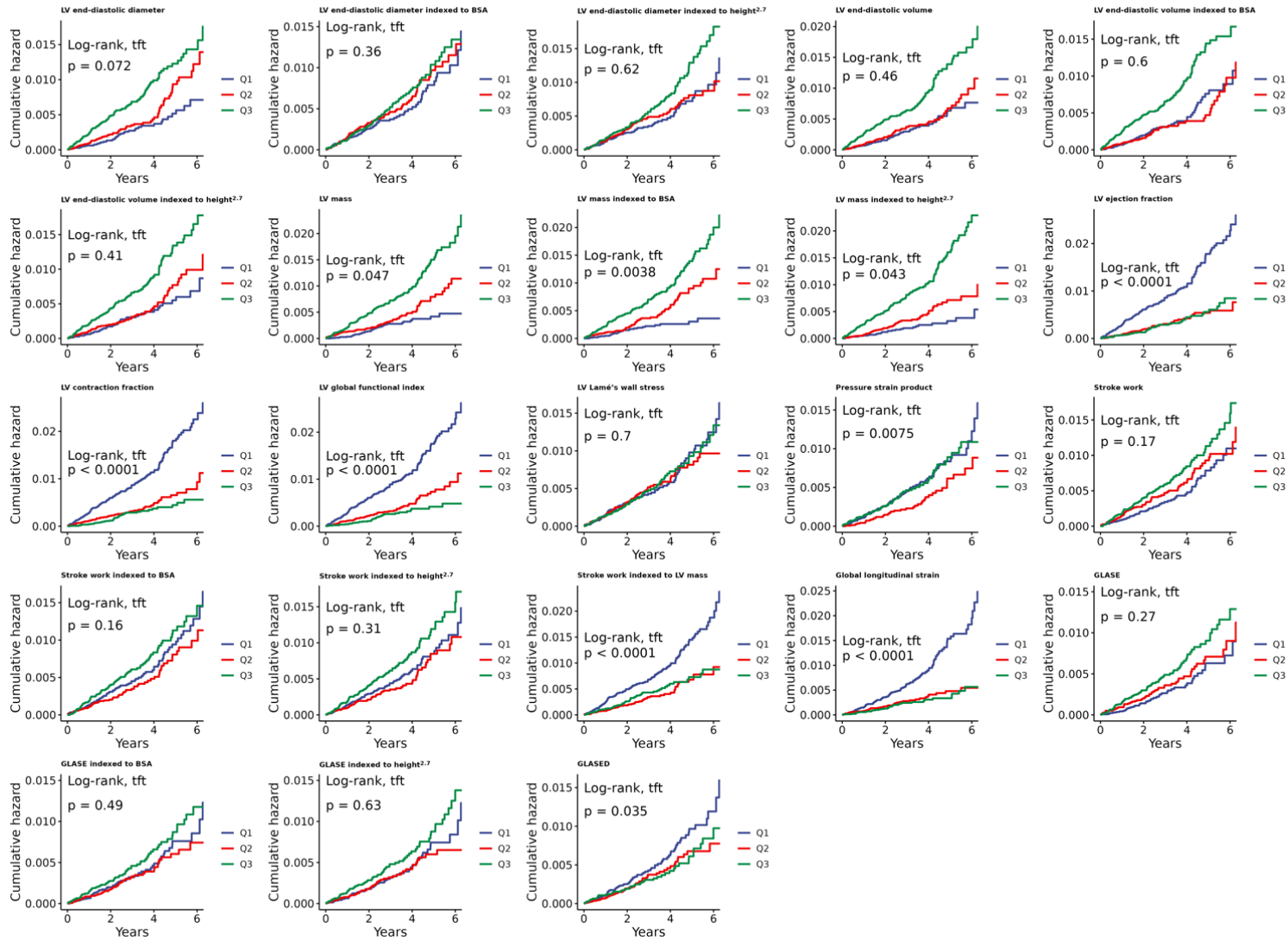


Table S1. The ICD10 codes used to define MACEs and heart failure

Condition	Coding	Meaning
MACE	I21	I21 Acute myocardial infarction
MACE	I210	I21.0 Acute transmural myocardial infarction of anterior wall
MACE	I211	I21.1 Acute transmural myocardial infarction of inferior wall
MACE	I212	I21.2 Acute transmural myocardial infarction of other sites
MACE	I213	I21.3 Acute transmural myocardial infarction of unspecified site
MACE	I214	I21.4 Acute subendocardial myocardial infarction
MACE	I219	I21.9 Acute myocardial infarction, unspecified
MACE	I21X	I21.X Presumed acute myocardial infarction (unconfirmed)
MACE	I22	I22 Subsequent myocardial infarction
MACE	I220	I22.0 Subsequent myocardial infarction of anterior wall
MACE	I221	I22.1 Subsequent myocardial infarction of inferior wall
MACE	I228	I22.8 Subsequent myocardial infarction of other sites
MACE	I229	I22.9 Subsequent myocardial infarction of unspecified site
MACE	I23	I23 Certain current complications following acute myocardial infarction
MACE	I230	I23.0 Haemopericardium as current complication following acute myocardial infarction
MACE	I231	I23.1 Atrial septal defect as current complication following acute myocardial infarction
MACE	I232	I23.2 Ventricular septal defect as current complication following acute myocardial infarction
MACE	I233	I23.3 Rupture of cardiac wall without haemopericardium as current complication following acute myocardial infarction
MACE	I234	I23.4 Rupture of chordae tendineae as current complication following acute myocardial infarction
MACE	I235	I23.5 Rupture of papillary muscle as current complication following acute myocardial infarction
MACE	I236	I23.6 Thrombosis of atrium, auricular appendage and ventricle as current complications following acute myocardial infarction
MACE	I238	I23.8 Other current complications following acute myocardial infarction
MACE	I24	I24 Other acute ischaemic heart diseases
MACE	I240	I24.0 Coronary thrombosis not resulting in myocardial infarction
MACE	I241	I24.1 Dressler's syndrome
MACE	I248	I24.8 Other forms of acute ischaemic heart disease
MACE	I249	I24.9 Acute ischaemic heart disease, unspecified
MACE	I25	I25 Chronic ischaemic heart disease
MACE	I250	I25.0 Atherosclerotic cardiovascular disease, so described
MACE	I251	I25.1 Atherosclerotic heart disease
MACE	I252	I25.2 Old myocardial infarction
MACE	I253	I25.3 Aneurysm of heart
MACE	I254	I25.4 Coronary artery aneurysm
MACE	I255	I25.5 Ischaemic cardiomyopathy
MACE	I256	I25.6 Silent myocardial ischaemia
MACE	I258	I25.8 Other forms of chronic ischaemic heart disease
MACE	I630	I63.0 Cerebral infarction due to thrombosis of precerebral arteries
MACE	I631	I63.1 Cerebral infarction due to embolism of precerebral arteries
MACE	I632	I63.2 Cerebral infarction due to unspecified occlusion or stenosis of precerebral arteries
MACE	I633	I63.3 Cerebral infarction due to thrombosis of cerebral arteries
MACE	I634	I63.4 Cerebral infarction due to embolism of cerebral arteries

MACE	I635	I63.5 Cerebral infarction due to unspecified occlusion or stenosis of cerebral arteries
MACE	I636	I63.6 Cerebral infarction due to cerebral venous thrombosis, nonpyogenic
MACE	I638	I63.8 Other cerebral infarction
MACE	I639	I63.9 Cerebral infarction, unspecified
MACE	I64	I64 Stroke, not specified as haemorrhage or infarction
MACE	I650	I65.0 Occlusion and stenosis of vertebral artery
MACE	I651	I65.1 Occlusion and stenosis of basilar artery
MACE	I652	I65.2 Occlusion and stenosis of carotid artery
MACE	I653	I65.3 Occlusion and stenosis of multiple and bilateral precerebral arteries
MACE	I658	I65.8 Occlusion and stenosis of other precerebral artery
MACE	I659	I65.9 Occlusion and stenosis of unspecified precerebral artery
MACE	I660	I66.0 Occlusion and stenosis of middle cerebral artery
MACE	I661	I66.1 Occlusion and stenosis of anterior cerebral artery
MACE	I662	I66.2 Occlusion and stenosis of posterior cerebral artery
MACE	I663	I66.3 Occlusion and stenosis of cerebellar arteries
MACE	I664	I66.4 Occlusion and stenosis of multiple and bilateral cerebral arteries
MACE	I668	I66.8 Occlusion and stenosis of other cerebral artery
MACE	I669	I66.9 Occlusion and stenosis of unspecified cerebral artery
MACE	I693	I69.3 Sequelae of cerebral infarction
HF	I110	I11.0 Hypertensive heart disease with (congestive) heart failure
HF	I130	I13.0 Hypertensive heart and renal disease with (congestive) heart failure
HF	I132	I13.2 Hypertensive heart and renal disease with both (congestive) heart failure and renal failure
HF	I500	I50.0 Congestive heart failure
HF	I501	I50.1 Left ventricular failure
HF	I509	I50.9 Heart failure, unspecified
HF	J81	J81 Pulmonary oedema

MACE, major adverse cardiovascular events; HF, heart failure

Table S2A. Demographics and main results (n=44,957)

	Mean (SD) or n(%)	Median [min, max]
Age (years)	64.1 (7.7)	65.0 [44.0, 82.0]
Sex		
Male	21631 (48.1%)	
Female	23326 (51.9%)	
Self-reported ethnicity		
White	43503 (96.8%)	
Asian	484 (1.1%)	
Chinese	131 (0.3%)	
Black	293 (0.7%)	
Mixed	216 (0.5%)	
Other	235 (0.5%)	
Height (m)	1.7 (0.1)	1.7 [1.3, 2.0]
Weight (kg)	75.9 (15.1)	74.5 [34.3, 185.0]
Body mass index (kg/m ²)	26.5 (4.4)	25.8 [14.1, 69.6]
Body surface area (m ²)	1.9 (0.2)	1.9 [1.2, 2.9]
Systolic blood pressure (mmHg)	139.1 (18.7)	137.5 [61.0, 240.5]
Diastolic blood pressure (mmHg)	77.8 (10.5)	77.5 [40.0, 169.0]
Heart rate (bpm)	68.0 (11.5)	67.0 [45.0, 156.5]
Ever smoked		
No	20640 (45.9%)	
Yes	23854 (53.1%)	
Physical activity (Total MET minutes per week)	2750.2 (2439.3)	2039.5 [0.0, 19278.0]
LV end-diastolic wall thickness (mm)	7.6 (1.1)	7.5 [4.6, 18.4]
LV end-diastolic diameter (mm)	52.0 (4.6)	51.8 [33.8, 80.8]
LV end-diastolic diameter indexed to BSA (mm/m ²)	28.1 (2.8)	28.1 [17.1, 45.5]
LV end-diastolic diameter indexed to height ^{2.7} (mm/m ^{2.7})	12.7 (1.6)	12.6 [7.6, 23.1]
LV end-diastolic volume (ml)	147.1 (33.8)	142.8 [43.1, 453.1]
LV end-diastolic volume indexed to BSA (ml/m ²)	78.8 (14.1)	77.4 [29.3, 238.8]
LV end-diastolic volume indexed to height ^{2.7} (ml/m ^{2.7})	35.4 (6.2)	34.8 [15.1, 101.6]
LV mass (g)	86.0 (22.4)	82.7 [28.5, 287.5]
LV mass indexed to BSA (g/m ²)	45.8 (8.7)	44.7 [17.4, 144.9]
LV mass indexed to height ^{2.7} (g/m ^{2.7})	20.6 (4.0)	20.1 [8.0, 62.6]
LV ejection fraction (%)	59.5 (6.2)	59.7 [11.7, 82.4]
LV contraction fraction (SV/LVMV)	109.0 (20.0)	108.2 [19.7, 277.0]
LV global function index	33.9 (4.5)	33.9 [6.1, 51.9]
LV Lamé's wall stress (Pa)	28078.7 (4578.0)	27835.6 [8858.6, 53223.4]
Pressure-strain product (mmHg%)	2511.8 (415.8)	2483.2 [1066.0, 4633.4]
Stroke work (mmHgml)	12133.8 (3308.1)	11723.7 [2006.0, 40981.3]
Stroke work indexed to BSA (mmHgml/m ²)	6498.5 (1519.1)	6333.9 [987.6, 18908.3]
Stroke work indexed to height ^{2.7} (mmHgml/m ^{2.7})	2925.6 (710.8)	2846.2 [420.3, 9221.3]
Stroke work indexed to LV mass (mmHgml/g)	143.4 (28.7)	141.2 [25.2, 345.7]
Global longitudinal strain (GLS) (-%)	18.1 (2.0)	18.1 [12.4, 23.7]
GLASE (kJ)	204.8 (57.3)	197.6 [47.8, 733.2]
GLASE indexed to BSA (kJ/m ²)	109.9 (26.9)	107.1 [32.5, 336.9]
GLASE indexed to height ^{2.7} (kJ/m ^{2.7})	49.4 (12.5)	48.1 [15.5, 161.8]
GLASED (kJ/m ³)	2.6 (0.6)	2.5 [0.8, 5.8]

Table S2B. Baseline characteristics stratified by cardiovascular disease status

	Pre-existing cardiovascular disease		P value
	No (N=41091)	Yes (N=3866)	
Age (years)			
Mean (SD)	63.7 (7.69)	68.4 (6.85)	<0.001
Median [Min, Max]	64.0 [44.0, 82.0]	69.0 [46.0, 82.0]	
Sex			
Male	18945 (46.1%)	2686 (69.5%)	<0.001
Female	22146 (53.9%)	1180 (30.5%)	
Self-reported ethnicity			
White	39749 (96.7%)	3754 (97.1%)	0.00173
Asian	428 (1.0%)	56 (1.4%)	
Chinese	126 (0.3%)	5 (0.1%)	
Black	281 (0.7%)	12 (0.3%)	
Mixed	203 (0.5%)	13 (0.3%)	
Other	218 (0.5%)	17 (0.4%)	
Height (m)			
Mean (SD)	1.69 (0.0926)	1.71 (0.0898)	<0.001
Median [Min, Max]	1.69 [1.34, 2.04]	1.72 [1.44, 1.97]	
Weight (kg)			
Mean (SD)	75.5 (15.0)	80.5 (15.0)	<0.001
Median [Min, Max]	74.0 [34.3, 185]	79.2 [39.6, 170]	
Body mass index (kg/m²)			
Mean (SD)	26.4 (4.36)	27.5 (4.45)	<0.001
Median [Min, Max]	25.8 [14.1, 69.6]	26.8 [14.5, 55.1]	
Body surface area (m²)			
Mean (SD)	1.85 (0.206)	1.92 (0.199)	<0.001
Median [Min, Max]	1.84 [1.21, 2.86]	1.92 [1.36, 2.81]	
Systolic blood pressure (mmHg)			
Mean (SD)	139 (18.6)	141 (18.7)	<0.001
Median [Min, Max]	138 [61.0, 241]	140 [62.0, 215]	
Diastolic blood pressure (mmHg)			
Mean (SD)	77.9 (10.5)	76.6 (10.2)	<0.001
Median [Min, Max]	77.5 [40.0, 169]	76.5 [41.0, 115]	
Heart rate (bpm)			
Mean (SD)	68.3 (11.4)	65.4 (11.8)	<0.001
Median [Min, Max]	67.0 [45.0, 157]	64.0 [45.0, 125]	
Ever smoked			
No	19095 (46.5%)	1545 (40.0%)	<0.001
Yes	21590 (52.5%)	2264 (58.6%)	
Physical activity (Total MET minutes per week)			
Mean (SD)	2760 (2440)	2640 (2430)	0.00369
Median [Min, Max]	2060 [0, 19300]	1920 [0, 17900]	
Hypertension			
No	29246 (71.2%)	1178 (30.5%)	<0.001
Yes	11845 (28.8%)	2688 (69.5%)	
Diabetes mellitus			
No	38924 (94.7%)	3336 (86.3%)	<0.001
Yes	2167 (5.3%)	530 (13.7%)	
Hyperlipidaemia			
No	28091 (68.4%)	854 (22.1%)	<0.001
Yes	13000 (31.6%)	3012 (77.9%)	
LV end-diastolic wall thickness (mm)			
Mean (SD)	7.52 (1.11)	8.11 (1.19)	<0.001
Median [Min, Max]	7.42 [4.64, 14.7]	8.04 [5.18, 18.4]	
LV end-diastolic diameter (mm)			
Mean (SD)	51.9 (4.48)	53.6 (5.11)	<0.001
Median [Min, Max]	51.6 [33.8, 78.4]	53.3 [38.9, 80.8]	
LV end-diastolic diameter indexed to BSA (mm/m²)			
Mean (SD)	28.2 (2.74)	28.0 (2.92)	0.00613
Median [Min, Max]	28.1 [17.8, 45.5]	27.9 [17.1, 42.3]	

LV end-diastolic diameter indexed to height^{2.7} (mm/m^{2.7})			
Mean (SD)	12.7 (1.60)	12.7 (1.70)	0.797
Median [Min, Max]	12.6 [7.55, 23.1]	12.5 [7.99, 20.5]	
LV end-diastolic volume (ml)			
Mean (SD)	146 (33.2)	157 (38.1)	<0.001
Median [Min, Max]	142 [43.1, 438]	153 [63.5, 453]	
LV end-diastolic volume indexed to BSA (ml/m²)			
Mean (SD)	78.5 (13.8)	81.6 (16.9)	<0.001
Median [Min, Max]	77.2 [29.3, 219]	79.9 [40.4, 239]	
LV end-diastolic volume indexed to height^{2.7} (ml/m^{2.7})			
Mean (SD)	35.2 (6.00)	36.8 (7.55)	<0.001
Median [Min, Max]	34.7 [15.1, 96.6]	36.1 [19.4, 102]	
LV mass (g)			
Mean (SD)	85.1 (22.0)	94.9 (23.8)	<0.001
Median [Min, Max]	81.6 [28.5, 248]	93.1 [39.5, 288]	
LV mass indexed to BSA (g/m²)			
Mean (SD)	45.5 (8.50)	49.0 (9.72)	<0.001
Median [Min, Max]	44.3 [17.4, 145]	48.1 [23.4, 130]	
LV mass indexed to height^{2.7} (g/m^{2.7})			
Mean (SD)	20.4 (3.88)	22.2 (4.56)	<0.001
Median [Min, Max]	20.0 [8.01, 62.6]	21.6 [10.8, 62.6]	
LV ejection fraction (%)			
Mean (SD)	59.7 (5.97)	57.6 (7.83)	<0.001
Median [Min, Max]	59.8 [13.4, 81.1]	58.4 [11.7, 82.4]	
LV contraction fraction (SV/LVMV)			
Mean (SD)	110 (19.8)	102 (20.4)	<0.001
Median [Min, Max]	109 [19.7, 277]	101 [24.5, 175]	
LV global functional index			
Mean (SD)	34.1 (4.35)	32.4 (5.22)	<0.001
Median [Min, Max]	34.0 [6.33, 52.0]	32.7 [6.08, 48.1]	
LV Lamé's wall stress (Pa)			
Mean (SD)	28200 (4540)	27200 (4930)	<0.001
Median [Min, Max]	27900 [11100, 53200]	27100 [8860, 46100]	
Pressure-strain product (mmHg%)			
Mean (SD)	2520 (413)	2470 (440)	<0.001
Median [Min, Max]	2480 [1070, 4630]	2460 [1130, 4060]	
Stroke work (mmHgml)			
Mean (SD)	12100 (3290)	12600 (3500)	<0.001
Median [Min, Max]	11700 [2010, 37100]	12400 [3190, 41000]	
Stroke work indexed to BSA (mmHgml/m²)			
Mean (SD)	6490 (1500)	6580 (1660)	0.00247
Median [Min, Max]	6320 [988, 18900]	6470 [1810, 18800]	
Stroke work indexed to height^{2.7} (mmHgml/m^{2.7})			
Mean (SD)	2920 (704)	2970 (781)	<0.001
Median [Min, Max]	2840 [420, 9220]	2910 [775, 9040]	
Stroke work indexed to LV mass (mmHgml/g)			
Mean (SD)	144 (28.4)	136 (30.5)	<0.001
Median [Min, Max]	142 [25.2, 346]	134 [30.7, 268]	
Global longitudinal strain (GLS) (%)			
Mean (SD)	18.1 (2.02)	17.6 (2.22)	<0.001
Median [Min, Max]	18.2 [12.4, 23.7]	17.6 [12.4, 23.6]	
GLASE (kJ)			
Mean (SD)	204 (57.0)	212 (60.5)	<0.001
Median [Min, Max]	197 [47.8, 601]	206 [53.4, 733]	
GLASE indexed to BSA (kJ/m²)			
Mean (SD)	110 (26.7)	110 (29.0)	0.212
Median [Min, Max]	107 [32.5, 305]	108 [34.0, 337]	
GLASE indexed to height^{2.7} (kJ/m^{2.7})			
Mean (SD)	49.4 (12.4)	49.9 (13.5)	0.0296
Median [Min, Max]	48.1 [15.5, 130]	48.6 [16.9, 162]	
GLASED (kJ/m³)			
Mean (SD)	2.57 (0.550)	2.42 (0.576)	<0.001
Median [Min, Max]	2.54 [0.838, 5.79]	2.39 [0.971, 4.67]	

Cardiovascular disease status was ascertained from self-reported medical history taken at the time of the visit to the imaging centre and included angina, heart attack/myocardial infarction, heart failure/pulmonary oedema, arrhythmias, stroke, peripheral vascular disease, valvular heart disease, cardiomyopathy and pericardial disease and prevalent MACE and heart failure identified from hospital episode statistics (Table S1).

Table S3A. Cox regression analysis of potential prognostic markers for all-cause mortality (Holm–Bonferroni corrected $P < 0.05$ in bold)

LV marker	Model 1		Model 2		C-statistic
	Hazard ratio (95% CI)	P value	Hazard ratio (95% CI)	P value	
↑ LV end-diastolic diameter	1.02 (1.00 to 1.04)	0.109	1.02 (1.00 to 1.05)	0.051	0.787
↓ LV end-diastolic diameter indexed to BSA	1.00 (0.97 to 1.04)	0.818	1.05 (1.00 to 1.09)	0.044	0.787
↑ LV end-diastolic diameter indexed to height ^{2.7}	1.02 (0.95 to 1.10)	0.552	1.04 (0.97 to 1.13)	0.249	0.789
↑ LV end-diastolic volume	1.00 (1.00 to 1.01)	0.033	1.00 (1.00 to 1.01)	0.030	0.789
↑ LV end-diastolic volume indexed to BSA	1.00 (1.00 to 1.01)	0.165	1.01 (1.00 to 1.02)	0.016	0.790
↑ LV end-diastolic volume indexed to height ^{2.7}	1.01 (1.00 to 1.03)	0.044	1.02 (1.00 to 1.03)	0.021	0.790
↑ LV mass	1.01 (1.01 to 1.02)	<0.0001	1.01 (1.00 to 1.02)	0.002	0.788
↑ LV mass indexed to BSA	1.02 (1.01 to 1.03)	0.0001	1.02 (1.01 to 1.03)	0.001	0.788
↑ LV mass indexed to height ^{2.7}	1.05 (1.02 to 1.07)	<0.0001	1.04 (1.02 to 1.07)	0.002	0.787
↓ LV ejection fraction	1.03 (1.01 to 1.04)	0.0001	1.03 (1.01 to 1.04)	0.0001	0.787
↓ LV contraction fraction (SV/LVMV)	1.01 (1.01 to 1.02)	<0.0001	1.01 (1.00 to 1.02)	0.001	0.793
↓ LV global function index	1.05 (1.03 to 1.07)	<0.0001	1.05 (1.02 to 1.07)	<0.0001	0.790
↓ LV Lamé's wall stress	1.00 (1.00 to 1.00)	0.059	1.00 (1.00 to 1.00)	0.476	0.786
↓ Pressure-strain product	1.00 (1.00 to 1.00)	0.118	1.00 (1.00 to 1.00)	0.087	0.788
↓ Stroke work	1.00 (1.00 to 1.00)	0.658	1.00 (1.00 to 1.00)	0.439	0.788
↓ Stroke work indexed to BSA	1.00 (1.00 to 1.00)	0.240	1.00 (1.00 to 1.00)	0.408	0.789
↓ Stroke work indexed to height ^{2.7}	1.00 (1.00 to 1.00)	0.460	1.00 (1.00 to 1.00)	0.361	0.790
↓ Stroke work indexed to LV mass	1.01 (1.00 to 1.01)	0.0002	1.01 (1.00 to 1.01)	0.005	0.791
↓ Global longitudinal strain	1.09 (1.04 to 1.15)	0.0007	1.09 (1.03 to 1.15)	0.001	0.792
↓ GLASE	1.00 (1.00 to 1.00)	0.480	1.00 (1.00 to 1.00)	0.436	0.787
↓ GLASE indexed to BSA	1.00 (1.00 to 1.01)	0.169	1.00 (1.00 to 1.01)	0.335	0.788
↓ GLASE indexed to height ^{2.7}	1.00 (1.00 to 1.01)	0.269	1.00 (1.00 to 1.01)	0.352	0.790
↓ GLASED	1.38 (1.13 to 1.68)	0.001	1.28 (1.04 to 1.57)	0.019	0.787

Model 1 was adjusted for age and sex, and Model 2 was adjusted for age, sex and cardiovascular risk factors (body mass index, hypertension, diabetes mellitus, dyslipidaemia, smoking history, regular alcohol intake, physical activity).

Table S3B. Cox regression analysis of potential prognostic markers for major adverse cardiovascular events (Holm–Bonferroni corrected $P < 0.05$ in bold)

LV marker	Model 1		Model 2		C-statistic
	Hazard ratio (95% CI)	P value	Hazard ratio (95% CI)	P value	
↑ LV end-diastolic diameter	1.03 (1.01 to 1.05)	0.0004	1.03 (1.02 to 1.05)	<0.0001	0.718
↓ LV end-diastolic diameter indexed to BSA	1.00 (0.97 to 1.03)	0.999	1.06 (1.03 to 1.10)	<0.0001	0.715
↑ LV end-diastolic diameter indexed to height ^{2.7}	1.11 (1.05 to 1.16)	<0.0001	1.10 (1.04 to 1.16)	0.0003	0.714
↑ LV end-diastolic volume	1.00 (1.00 to 1.01)	<0.0001	1.01 (1.00 to 1.01)	<0.0001	0.716
↑ LV end-diastolic volume indexed to BSA	1.01 (1.00 to 1.01)	0.003	1.01 (1.01 to 1.02)	<0.0001	0.714
↑ LV end-diastolic volume indexed to height ^{2.7}	1.03 (1.02 to 1.04)	<0.0001	1.03 (1.02 to 1.04)	<0.0001	0.714
↑ LV mass	1.02 (1.02 to 1.02)	<0.0001	1.02 (1.02 to 1.02)	<0.0001	0.732
↑ LV mass indexed to BSA	1.05 (1.04 to 1.06)	<0.0001	1.05 (1.04 to 1.05)	<0.0001	0.730
↑ LV mass indexed to height ^{2.7}	1.10 (1.09 to 1.12)	<0.0001	1.10 (1.08 to 1.12)	<0.0001	0.727
↓ LV ejection fraction	1.03 (1.02 to 1.04)	<0.0001	1.03 (1.02 to 1.04)	<0.0001	0.714
↓ LV contraction fraction (SV/LVMV)	1.02 (1.02 to 1.03)	<0.0001	1.02 (1.01 to 1.02)	<0.0001	0.729
↓ LV global function index	1.07 (1.05 to 1.08)	<0.0001	1.06 (1.04 to 1.08)	<0.0001	0.719
↓ LV Lamé's wall stress	1.00 (1.00 to 1.00)	0.004	1.00 (1.00 to 1.00)	0.259	0.715
↑ Pressure-strain product	1.00 (1.00 to 1.00)	0.664	1.00 (1.00 to 1.00)	0.825	0.715
↑ Stroke work	1.00 (1.00 to 1.00)	0.0008	1.00 (1.00 to 1.00)	0.007	0.714
↑ Stroke work indexed to BSA	1.00 (1.00 to 1.00)	0.019	1.00 (1.00 to 1.00)	0.004	0.713
↑ Stroke work indexed to height ^{2.7}	1.00 (1.00 to 1.00)	<0.0001	1.00 (1.00 to 1.00)	0.003	0.712
↓ Stroke work indexed to LV mass	1.01 (1.00 to 1.01)	<0.0001	1.01 (1.00 to 1.01)	<0.0001	0.720
↓ Global longitudinal strain	1.12 (1.08 to 1.16)	<0.0001	1.10 (1.06 to 1.14)	<0.0001	0.712
↑ GLASE	1.00 (1.00 to 1.00)	0.021	1.00 (1.00 to 1.00)	0.028	0.717
↑ GLASE indexed to BSA	1.00 (1.00 to 1.00)	0.192	1.00 (1.00 to 1.01)	0.022	0.716
↑ GLASE indexed to height ^{2.7}	1.01 (1.00 to 1.01)	0.004	1.01 (1.00 to 1.01)	0.016	0.716
↓ GLASED	1.39 (1.21 to 1.61)	<0.0001	1.25 (1.08 to 1.44)	0.003	0.717

Model 1 was adjusted for age and sex, and Model 2 was adjusted for age, sex and cardiovascular risk factors (body mass index, hypertension, diabetes mellitus, dyslipidaemia, smoking history, regular alcohol intake, physical activity).

Table S3C. Cox regression analysis of potential prognostic markers for heart failure (Holm–Bonferroni corrected $P < 0.05$ in bold)

LV marker	Model 1		Model 2		C-statistic
	Hazard ratio (95% CI)	P value	Hazard ratio (95% CI)	P value	
↑ LV end-diastolic diameter	1.16 (1.14 to 1.19)	<0.0001	1.16 (1.13 to 1.19)	<0.0001	0.779
↑ LV end-diastolic diameter indexed to BSA	1.15 (1.10 to 1.20)	<0.0001	1.29 (1.23 to 1.35)	<0.0001	0.720
↑ LV end-diastolic diameter indexed to height ^{2.7}	1.45 (1.33 to 1.57)	<0.0001	1.40 (1.28 to 1.53)	<0.0001	0.699
↑ LV end-diastolic volume	1.02 (1.01 to 1.02)	<0.0001	1.02 (1.01 to 1.02)	<0.0001	0.760
↑ LV end-diastolic volume indexed to BSA	1.03 (1.03 to 1.04)	<0.0001	1.04 (1.03 to 1.04)	<0.0001	0.748
↑ LV end-diastolic volume indexed to height ^{2.7}	1.08 (1.07 to 1.10)	<0.0001	1.08 (1.07 to 1.09)	<0.0001	0.734
↑ LV mass	1.03 (1.03 to 1.03)	<0.0001	1.03 (1.02 to 1.03)	<0.0001	0.743
↑ LV mass indexed to BSA	1.06 (1.05 to 1.07)	<0.0001	1.06 (1.05 to 1.07)	<0.0001	0.730
↑ LV mass indexed to height ^{2.7}	1.14 (1.13 to 1.16)	<0.0001	1.14 (1.12 to 1.16)	<0.0001	0.713
↓ LV ejection fraction	1.11 (1.10 to 1.13)	<0.0001	1.11 (1.09 to 1.12)	<0.0001	0.786
↓ LV contraction fraction (SV/LVMV)	1.04 (1.03 to 1.05)	<0.0001	1.03 (1.02 to 1.04)	<0.0001	0.735
↓ LV global function index	1.19 (1.16 to 1.21)	<0.0001	1.17 (1.15 to 1.20)	<0.0001	0.773
↑ LV Lamé's wall stress	1.00 (1.00 to 1.00)	0.322	1.00 (1.00 to 1.00)	0.026	0.731
↓ Pressure-strain product	1.00 (1.00 to 1.00)	0.002	1.00 (1.00 to 1.00)	0.0002	0.748
↑ Stroke work	1.00 (1.00 to 1.00)	0.043	1.00 (1.00 to 1.00)	0.392	0.707
↑ Stroke work indexed to BSA	1.00 (1.00 to 1.00)	0.555	1.00 (1.00 to 1.00)	0.438	0.702
↑ Stroke work indexed to height ^{2.7}	1.00 (1.00 to 1.00)	0.017	1.00 (1.00 to 1.00)	0.459	0.699
↓ Stroke work indexed to LV mass	1.02 (1.01 to 1.02)	<0.0001	1.02 (1.01 to 1.02)	<0.0001	0.728
↓ Global longitudinal strain	1.30 (1.21 to 1.40)	<0.0001	1.28 (1.19 to 1.38)	<0.0001	0.793
↑ GLASE	1.00 (1.00 to 1.01)	0.0007	1.00 (1.00 to 1.01)	0.005	0.708
↑ GLASE indexed to BSA	1.01 (1.00 to 1.01)	0.005	1.01 (1.00 to 1.01)	0.003	0.703
↑ GLASE indexed to height ^{2.7}	1.02 (1.01 to 1.03)	<0.0001	1.02 (1.01 to 1.03)	0.003	0.700
↓ GLASED	1.41 (1.06 to 1.88)	0.019	1.24 (0.93 to 1.67)	0.147	0.726

Model 1 was adjusted for age and sex, and Model 2 was adjusted for age, sex and cardiovascular risk factors (body mass index, hypertension, diabetes mellitus, dyslipidaemia, smoking history, regular alcohol intake, physical activity).

Table S4. Comparison of hazard ratios according to GLASED vs other potential prognostic markers

Model	Outcome	Marker 1 (P1)	Marker 2 (P2)	P1 Hazard ratio (95% CI)	P1 P value	P2 Hazard ratio (95% CI)	P2 P value	Comparison P value* (P1 vs P2 HR)
Model 1	All-cause mortality	↓ GLASED	↓ Global longitudinal strain	1.38 (1.13 to 1.68)	0.001	1.09 (1.04 to 1.15)	7e-04	<0.0001
		↓ GLASED	↓ LV global functional index	1.38 (1.13 to 1.68)	0.001	1.05 (1.03 to 1.07)	<0.0001	<0.0001
		↓ GLASED	↑ LV mass indexed to height ^{2.7}	1.38 (1.13 to 1.68)	0.001	1.05 (1.02 to 1.07)	<0.0001	<0.0001
		↓ GLASED	↓ LV ejection fraction	1.38 (1.13 to 1.68)	0.001	1.03 (1.01 to 1.04)	1e-04	<0.0001
		↓ GLASED	↑ LV mass indexed to BSA	1.38 (1.13 to 1.68)	0.001	1.02 (1.01 to 1.03)	1e-04	<0.0001
		↓ GLASED	↑ LV end-diastolic diameter	1.38 (1.13 to 1.68)	0.001	1.02 (1.00 to 1.04)	0.109	<0.0001
		↓ GLASED	↑ LV end-diastolic diameter indexed to height ^{2.7}	1.38 (1.13 to 1.68)	0.001	1.02 (0.95 to 1.10)	0.552	<0.0001
		↓ GLASED	↑ LV mass	1.38 (1.13 to 1.68)	0.001	1.01 (1.01 to 1.02)	<0.0001	<0.0001
		↓ GLASED	↓ LV contraction fraction	1.38 (1.13 to 1.68)	0.001	1.01 (1.01 to 1.02)	<0.0001	<0.0001
		↓ GLASED	↑ LV end-diastolic volume indexed to height ^{2.7}	1.38 (1.13 to 1.68)	0.001	1.01 (1.00 to 1.03)	0.044	<0.0001
		↓ GLASED	↓ Stroke work indexed to LV mass	1.38 (1.13 to 1.68)	0.001	1.01 (1.00 to 1.01)	2e-04	<0.0001
		↓ GLASED	↑ LV end-diastolic volume	1.38 (1.13 to 1.68)	0.001	1.00 (1.00 to 1.01)	0.033	<0.0001
		↓ GLASED	↑ LV end-diastolic volume indexed to BSA	1.38 (1.13 to 1.68)	0.001	1.00 (1.00 to 1.01)	0.165	<0.0001
		↓ GLASED	↓ GLASE indexed to BSA	1.38 (1.13 to 1.68)	0.001	1.00 (1.00 to 1.01)	0.169	<0.0001
		↓ GLASED	↓ GLASE indexed to height ^{2.7}	1.38 (1.13 to 1.68)	0.001	1.00 (1.00 to 1.01)	0.269	<0.0001
		↓ GLASED	↓ LV Lamé's wall stress	1.38 (1.13 to 1.68)	0.001	1.00 (1.00 to 1.00)	0.059	<0.0001
		↓ GLASED	↓ Pressure-strain product	1.38 (1.13 to 1.68)	0.001	1.00 (1.00 to 1.00)	0.118	<0.0001
		↓ GLASED	↓ Stroke work	1.38 (1.13 to 1.68)	0.001	1.00 (1.00 to 1.00)	0.658	<0.0001
		↓ GLASED	↓ Stroke work indexed to BSA	1.38 (1.13 to 1.68)	0.001	1.00 (1.00 to 1.00)	0.240	<0.0001
		↓ GLASED	↓ Stroke work indexed to height ^{2.7}	1.38 (1.13 to 1.68)	0.001	1.00 (1.00 to 1.00)	0.460	<0.0001
		↓ GLASED	↓ GLASE	1.38 (1.13 to 1.68)	0.001	1.00 (1.00 to 1.00)	0.480	<0.0001
↓ GLASED	↓ LV end-diastolic diameter indexed to BSA	1.38 (1.13 to 1.68)	0.001	1.00 (0.97 to 1.04)	0.818	<0.0001		
Model 2	↓ GLASED	↓ Global longitudinal strain	1.28 (1.04 to 1.57)	0.019	1.09 (1.03 to 1.15)	0.001	<0.0001	
	↓ GLASED	↓ LV global functional index	1.28 (1.04 to 1.57)	0.019	1.05 (1.02 to 1.07)	<0.0001	<0.0001	

		↓ GLASED	↑ LV end-diastolic diameter indexed to BSA	1.28 (1.04 to 1.57)	0.019	1.05 (1.00 to 1.09)	0.044	<0.0001
		↓ GLASED	↑ LV mass indexed to height ^{2.7}	1.28 (1.04 to 1.57)	0.019	1.04 (1.02 to 1.07)	0.002	<0.0001
		↓ GLASED	↑ LV end-diastolic diameter indexed to height ^{2.7}	1.28 (1.04 to 1.57)	0.019	1.04 (0.97 to 1.13)	0.249	<0.0001
		↓ GLASED	↓ LV ejection fraction	1.28 (1.04 to 1.57)	0.019	1.03 (1.01 to 1.04)	1e-04	<0.0001
		↓ GLASED	↑ LV mass indexed to BSA	1.28 (1.04 to 1.57)	0.019	1.02 (1.01 to 1.03)	0.001	<0.0001
		↓ GLASED	↑ LV end-diastolic diameter	1.28 (1.04 to 1.57)	0.019	1.02 (1.00 to 1.05)	0.051	<0.0001
		↓ GLASED	↑ LV end-diastolic volume indexed to height ^{2.7}	1.28 (1.04 to 1.57)	0.019	1.02 (1.00 to 1.03)	0.021	<0.0001
		↓ GLASED	↑ LV end-diastolic volume indexed to BSA	1.28 (1.04 to 1.57)	0.019	1.01 (1.00 to 1.02)	0.016	<0.0001
		↓ GLASED	↑ LV mass	1.28 (1.04 to 1.57)	0.019	1.01 (1.00 to 1.02)	0.002	<0.0001
		↓ GLASED	↓ LV contraction fraction	1.28 (1.04 to 1.57)	0.019	1.01 (1.00 to 1.02)	0.001	<0.0001
		↓ GLASED	↓ Stroke work indexed to LV mass	1.28 (1.04 to 1.57)	0.019	1.01 (1.00 to 1.01)	0.005	<0.0001
		↓ GLASED	↑ LV end-diastolic volume	1.28 (1.04 to 1.57)	0.019	1.00 (1.00 to 1.01)	0.030	<0.0001
		↓ GLASED	↓ GLASE indexed to BSA	1.28 (1.04 to 1.57)	0.019	1.00 (1.00 to 1.01)	0.335	<0.0001
		↓ GLASED	↓ GLASE indexed to height ^{2.7}	1.28 (1.04 to 1.57)	0.019	1.00 (1.00 to 1.01)	0.352	<0.0001
		↓ GLASED	↓ LV Lamé's wall stress	1.28 (1.04 to 1.57)	0.019	1.00 (1.00 to 1.00)	0.476	<0.0001
		↓ GLASED	↓ Pressure-strain product	1.28 (1.04 to 1.57)	0.019	1.00 (1.00 to 1.00)	0.087	<0.0001
		↓ GLASED	↓ Stroke work	1.28 (1.04 to 1.57)	0.019	1.00 (1.00 to 1.00)	0.439	<0.0001
		↓ GLASED	↓ Stroke work indexed to BSA	1.28 (1.04 to 1.57)	0.019	1.00 (1.00 to 1.00)	0.408	<0.0001
		↓ GLASED	↓ Stroke work indexed to height ^{2.7}	1.28 (1.04 to 1.57)	0.019	1.00 (1.00 to 1.00)	0.361	<0.0001
		↓ GLASED	↓ GLASE	1.28 (1.04 to 1.57)	0.019	1.00 (1.00 to 1.00)	0.436	<0.0001
Model 1	MACE	↓ GLASED	↓ Global longitudinal strain	1.39 (1.21 to 1.61)	<0.0001	1.12 (1.08 to 1.16)	<0.0001	<0.0001
		↓ GLASED	↑ LV end-diastolic diameter indexed to height ^{2.7}	1.39 (1.21 to 1.61)	<0.0001	1.11 (1.06 to 1.16)	<0.0001	<0.0001
		↓ GLASED	↑ LV mass indexed to height ^{2.7}	1.39 (1.21 to 1.61)	<0.0001	1.10 (1.09 to 1.12)	<0.0001	<0.0001
		↓ GLASED	↓ LV global functional index	1.39 (1.21 to 1.61)	<0.0001	1.07 (1.05 to 1.09)	<0.0001	<0.0001
		↓ GLASED	↑ LV mass indexed to BSA	1.39 (1.21 to 1.61)	<0.0001	1.05 (1.04 to 1.06)	<0.0001	<0.0001
		↓ GLASED	↑ LV end-diastolic volume indexed to height ^{2.7}	1.39 (1.21 to 1.61)	<0.0001	1.03 (1.02 to 1.04)	<0.0001	<0.0001
		↓ GLASED	↓ LV ejection fraction	1.39 (1.21 to 1.61)	<0.0001	1.03 (1.02 to 1.04)	<0.0001	<0.0001
		↓ GLASED	↑ LV end-diastolic diameter	1.39 (1.21 to 1.61)	<0.0001	1.03 (1.01 to 1.05)	4e-04	<0.0001

	↓ GLASED	↓ LV contraction fraction	1.39 (1.21 to 1.61)	<0.0001	1.02 (1.02 to 1.03)	<0.0001	<0.0001
	↓ GLASED	↑ LV mass	1.39 (1.21 to 1.61)	<0.0001	1.02 (1.02 to 1.02)	<0.0001	<0.0001
	↓ GLASED	↑ LV end-diastolic volume indexed to BSA	1.39 (1.21 to 1.61)	<0.0001	1.01 (1.00 to 1.01)	0.003	<0.0001
	↓ GLASED	↓ Stroke work indexed to LV mass	1.39 (1.21 to 1.61)	<0.0001	1.01 (1.00 to 1.01)	<0.0001	<0.0001
	↓ GLASED	↑ GLASE indexed to height ^{2.7}	1.39 (1.21 to 1.61)	<0.0001	1.01 (1.00 to 1.01)	0.005	<0.0001
	↓ GLASED	↑ LV end-diastolic volume	1.39 (1.21 to 1.61)	<0.0001	1.00 (1.00 to 1.01)	<0.0001	<0.0001
	↓ GLASED	↓ LV Lamé's wall stress	1.39 (1.21 to 1.61)	<0.0001	1.00 (1.00 to 1.00)	0.004	<0.0001
	↓ GLASED	↑ Pressure-strain product	1.39 (1.21 to 1.61)	<0.0001	1.00 (1.00 to 1.00)	0.681	<0.0001
	↓ GLASED	↑ Stroke work	1.39 (1.21 to 1.61)	<0.0001	1.00 (1.00 to 1.00)	9e-04	<0.0001
	↓ GLASED	↑ Stroke work indexed to BSA	1.39 (1.21 to 1.61)	<0.0001	1.00 (1.00 to 1.00)	0.020	<0.0001
	↓ GLASED	↑ Stroke work indexed to height ^{2.7}	1.39 (1.21 to 1.61)	<0.0001	1.00 (1.00 to 1.00)	<0.0001	<0.0001
	↓ GLASED	↑ GLASE	1.39 (1.21 to 1.61)	<0.0001	1.00 (1.00 to 1.00)	0.022	<0.0001
	↓ GLASED	↑ GLASE indexed to BSA	1.39 (1.21 to 1.61)	<0.0001	1.00 (1.00 to 1.00)	0.196	<0.0001
	↓ GLASED	↑ LV end-diastolic diameter indexed to BSA	1.39 (1.21 to 1.61)	<0.0001	1.00 (0.97 to 1.03)	0.994	<0.0001
Model 2	↓ GLASED	↑ LV mass indexed to height ^{2.7}	1.25 (1.08 to 1.44)	0.003	1.10 (1.08 to 1.12)	<0.0001	<0.0001
	↓ GLASED	↓ Global longitudinal strain	1.25 (1.08 to 1.44)	0.003	1.10 (1.06 to 1.14)	<0.0001	<0.0001
	↓ GLASED	↑ LV end-diastolic diameter indexed to height ^{2.7}	1.25 (1.08 to 1.44)	0.003	1.10 (1.04 to 1.16)	3e-04	<0.0001
	↓ GLASED	↓ LV global functional index	1.25 (1.08 to 1.44)	0.003	1.06 (1.04 to 1.08)	<0.0001	<0.0001
	↓ GLASED	↑ LV end-diastolic diameter indexed to BSA	1.25 (1.08 to 1.44)	0.003	1.06 (1.03 to 1.10)	<0.0001	<0.0001
	↓ GLASED	↑ LV mass indexed to BSA	1.25 (1.08 to 1.44)	0.003	1.05 (1.04 to 1.05)	<0.0001	<0.0001
	↓ GLASED	↑ LV end-diastolic diameter	1.25 (1.08 to 1.44)	0.003	1.03 (1.02 to 1.05)	<0.0001	<0.0001
	↓ GLASED	↑ LV end-diastolic volume indexed to height ^{2.7}	1.25 (1.08 to 1.44)	0.003	1.03 (1.02 to 1.04)	<0.0001	<0.0001
	↓ GLASED	↓ LV ejection fraction	1.25 (1.08 to 1.44)	0.003	1.03 (1.02 to 1.04)	<0.0001	<0.0001
	↓ GLASED	↑ LV mass	1.25 (1.08 to 1.44)	0.003	1.02 (1.02 to 1.02)	<0.0001	<0.0001
	↓ GLASED	↓ LV contraction fraction	1.25 (1.08 to 1.44)	0.003	1.02 (1.01 to 1.02)	<0.0001	<0.0001
	↓ GLASED	↑ LV end-diastolic volume indexed to BSA	1.25 (1.08 to 1.44)	0.003	1.01 (1.01 to 1.02)	<0.0001	<0.0001
	↓ GLASED	↑ LV end-diastolic volume	1.25 (1.08 to 1.44)	0.003	1.01 (1.00 to 1.01)	<0.0001	<0.0001
	↓ GLASED	↓ Stroke work indexed to LV mass	1.25 (1.08 to 1.44)	0.003	1.01 (1.00 to 1.01)	<0.0001	<0.0001
	↓ GLASED	↑ GLASE indexed to height ^{2.7}	1.25 (1.08 to 1.44)	0.003	1.01 (1.00 to 1.01)	0.016	<0.0001

		↓ GLASED	↑ GLASE indexed to BSA	1.25 (1.08 to 1.44)	0.003	1.00 (1.00 to 1.01)	0.023	<0.0001
		↓ GLASED	↓ LV Lamé's wall stress	1.25 (1.08 to 1.44)	0.003	1.00 (1.00 to 1.00)	0.256	<0.0001
		↓ GLASED	↓ Pressure-strain product	1.25 (1.08 to 1.44)	0.003	1.00 (1.00 to 1.00)	0.812	<0.0001
		↓ GLASED	↑ Stroke work	1.25 (1.08 to 1.44)	0.003	1.00 (1.00 to 1.00)	0.008	<0.0001
		↓ GLASED	↑ Stroke work indexed to BSA	1.25 (1.08 to 1.44)	0.003	1.00 (1.00 to 1.00)	0.004	<0.0001
		↓ GLASED	↑ Stroke work indexed to height ^{2.7}	1.25 (1.08 to 1.44)	0.003	1.00 (1.00 to 1.00)	0.004	<0.0001
		↓ GLASED	↑ GLASE	1.25 (1.08 to 1.44)	0.003	1.00 (1.00 to 1.00)	0.028	<0.0001
Model 1	Heart failure	↓ GLASED	↑ LV end-diastolic diameter indexed to height ^{2.7}	1.41 (1.06 to 1.88)	0.018	1.45 (1.34 to 1.57)	<0.0001	ns
		↓ GLASED	↓ Global longitudinal strain	1.41 (1.06 to 1.88)	0.018	1.30 (1.21 to 1.40)	<0.0001	<0.0001
		↓ GLASED	↓ LV global functional index	1.41 (1.06 to 1.88)	0.018	1.19 (1.16 to 1.21)	<0.0001	<0.0001
		↓ GLASED	↑ LV end-diastolic diameter	1.41 (1.06 to 1.88)	0.018	1.17 (1.14 to 1.19)	<0.0001	<0.0001
		↓ GLASED	↑ LV end-diastolic diameter indexed to BSA	1.41 (1.06 to 1.88)	0.018	1.15 (1.10 to 1.20)	<0.0001	<0.0001
		↓ GLASED	↑ LV mass indexed to height ^{2.7}	1.41 (1.06 to 1.88)	0.018	1.14 (1.13 to 1.16)	<0.0001	<0.0001
		↓ GLASED	↓ LV ejection fraction	1.41 (1.06 to 1.88)	0.018	1.11 (1.10 to 1.13)	<0.0001	<0.0001
		↓ GLASED	↑ LV end-diastolic volume indexed to height ^{2.7}	1.41 (1.06 to 1.88)	0.018	1.09 (1.07 to 1.10)	<0.0001	<0.0001
		↓ GLASED	↑ LV mass indexed to BSA	1.41 (1.06 to 1.88)	0.018	1.06 (1.05 to 1.07)	<0.0001	<0.0001
		↓ GLASED	↓ LV contraction fraction	1.41 (1.06 to 1.88)	0.018	1.04 (1.03 to 1.05)	<0.0001	<0.0001
		↓ GLASED	↑ LV end-diastolic volume indexed to BSA	1.41 (1.06 to 1.88)	0.018	1.03 (1.03 to 1.04)	<0.0001	<0.0001
		↓ GLASED	↑ LV mass	1.41 (1.06 to 1.88)	0.018	1.03 (1.03 to 1.03)	<0.0001	<0.0001
		↓ GLASED	↑ LV end-diastolic volume	1.41 (1.06 to 1.88)	0.018	1.02 (1.02 to 1.02)	<0.0001	<0.0001
		↓ GLASED	↑ GLASE indexed to height ^{2.7}	1.41 (1.06 to 1.88)	0.018	1.02 (1.01 to 1.03)	<0.0001	<0.0001
		↓ GLASED	↓ Stroke work indexed to LV mass	1.41 (1.06 to 1.88)	0.018	1.02 (1.01 to 1.02)	<0.0001	<0.0001
		↓ GLASED	↑ GLASE indexed to BSA	1.41 (1.06 to 1.88)	0.018	1.01 (1.00 to 1.01)	0.005	<0.0001
		↓ GLASED	↑ GLASE	1.41 (1.06 to 1.88)	0.018	1.00 (1.00 to 1.01)	7e-04	<0.0001
		↓ GLASED	↑ LV Lamé's wall stress	1.41 (1.06 to 1.88)	0.018	1.00 (1.00 to 1.00)	0.329	<0.0001
		↓ GLASED	↓ Pressure-strain product	1.41 (1.06 to 1.88)	0.018	1.00 (1.00 to 1.00)	0.002	<0.0001
		↓ GLASED	↑ Stroke work	1.41 (1.06 to 1.88)	0.018	1.00 (1.00 to 1.00)	0.045	<0.0001
		↓ GLASED	↑ Stroke work indexed to BSA	1.41 (1.06 to 1.88)	0.018	1.00 (1.00 to 1.00)	0.567	<0.0001

Model 2	↓ GLASED	↑ Stroke work indexed to height ^{2.7}	1.41 (1.06 to 1.88)	0.018	1.00 (1.00 to 1.00)	0.017	<0.0001
	↓ GLASED	↑ LV end-diastolic diameter indexed to height ^{2.7}	1.25 (0.93 to 1.67)	0.145	1.40 (1.29 to 1.53)	<0.0001	<0.0001
	↓ GLASED	↑ LV end-diastolic diameter indexed to BSA	1.25 (0.93 to 1.67)	0.145	1.29 (1.23 to 1.35)	<0.0001	<0.01
	↓ GLASED	↓ Global longitudinal strain	1.25 (0.93 to 1.67)	0.145	1.28 (1.19 to 1.38)	<0.0001	ns
	↓ GLASED	↓ LV global functional index	1.25 (0.93 to 1.67)	0.145	1.18 (1.15 to 1.20)	<0.0001	<0.0001
	↓ GLASED	↑ LV end-diastolic diameter	1.25 (0.93 to 1.67)	0.145	1.16 (1.14 to 1.19)	<0.0001	<0.0001
	↓ GLASED	↑ LV mass indexed to height ^{2.7}	1.25 (0.93 to 1.67)	0.145	1.14 (1.12 to 1.16)	<0.0001	<0.0001
	↓ GLASED	↓ LV ejection fraction	1.25 (0.93 to 1.67)	0.145	1.11 (1.09 to 1.12)	<0.0001	<0.0001
	↓ GLASED	↑ LV end-diastolic volume indexed to height ^{2.7}	1.25 (0.93 to 1.67)	0.145	1.08 (1.07 to 1.10)	<0.0001	<0.0001
	↓ GLASED	↑ LV mass indexed to BSA	1.25 (0.93 to 1.67)	0.145	1.06 (1.05 to 1.07)	<0.0001	<0.0001
	↓ GLASED	↑ LV end-diastolic volume indexed to BSA	1.25 (0.93 to 1.67)	0.145	1.04 (1.03 to 1.04)	<0.0001	<0.0001
	↓ GLASED	↓ LV contraction fraction	1.25 (0.93 to 1.67)	0.145	1.03 (1.02 to 1.04)	<0.0001	<0.0001
	↓ GLASED	↑ LV mass	1.25 (0.93 to 1.67)	0.145	1.03 (1.02 to 1.03)	<0.0001	<0.0001
	↓ GLASED	↑ LV end-diastolic volume	1.25 (0.93 to 1.67)	0.145	1.02 (1.02 to 1.02)	<0.0001	<0.0001
	↓ GLASED	↑ GLASE indexed to height ^{2.7}	1.25 (0.93 to 1.67)	0.145	1.02 (1.01 to 1.03)	0.003	<0.0001
	↓ GLASED	↓ Stroke work indexed to LV mass	1.25 (0.93 to 1.67)	0.145	1.02 (1.01 to 1.02)	<0.0001	<0.0001
	↓ GLASED	↑ GLASE indexed to BSA	1.25 (0.93 to 1.67)	0.145	1.01 (1.00 to 1.01)	0.003	<0.0001
	↓ GLASED	↑ GLASE	1.25 (0.93 to 1.67)	0.145	1.00 (1.00 to 1.01)	0.005	<0.0001
	↓ GLASED	↑ LV Lamé's wall stress	1.25 (0.93 to 1.67)	0.145	1.00 (1.00 to 1.00)	0.026	<0.0001
	↓ GLASED	↓ Pressure-strain product	1.25 (0.93 to 1.67)	0.145	1.00 (1.00 to 1.00)	2e-04	<0.0001
	↓ GLASED	↑ Stroke work	1.25 (0.93 to 1.67)	0.145	1.00 (1.00 to 1.00)	0.407	<0.0001
↓ GLASED	↑ Stroke work indexed to BSA	1.25 (0.93 to 1.67)	0.145	1.00 (1.00 to 1.00)	0.451	<0.0001	
↓ GLASED	↑ Stroke work indexed to height ^{2.7}	1.25 (0.93 to 1.67)	0.145	1.00 (1.00 to 1.00)	0.471	<0.0001	

*Holm–Bonferroni-corrected *P* value

Table S5A. Cox regression analysis of potential prognostic markers for all-cause mortality in the subgroup with a normal LVEF (>55%)

LV marker	Model 1		Model 2	
	Hazard ratio (95% CI)	P value	Hazard ratio (95% CI)	P value
↓ LV end-diastolic diameter	1.01 (0.98 to 1.04)	0.592	1.00 (0.97 to 1.03)	0.901
↓ LV end-diastolic diameter indexed to BSA	1.04 (1.00 to 1.09)	0.080	1.01 (0.96 to 1.07)	0.700
↓ LV end-diastolic diameter indexed to height ^{2.7}	1.07 (0.98 to 1.17)	0.119	1.05 (0.95 to 1.15)	0.346
↓ LV end-diastolic volume	1.00 (1.00 to 1.01)	0.610	1.00 (1.00 to 1.01)	0.697
↓ LV end-diastolic volume indexed to BSA	1.01 (1.00 to 1.02)	0.176	1.00 (0.99 to 1.01)	0.550
↓ LV end-diastolic volume indexed to height ^{2.7}	1.01 (0.99 to 1.03)	0.239	1.01 (0.99 to 1.03)	0.403
↑ LV mass	1.01 (1.00 to 1.01)	0.029	1.01 (1.00 to 1.01)	0.122
↑ LV mass indexed to BSA	1.01 (1.00 to 1.03)	0.104	1.01 (1.00 to 1.03)	0.159
↑ LV mass indexed to height ^{2.7}	1.02 (0.99 to 1.06)	0.124	1.02 (0.98 to 1.06)	0.271
↓ LV ejection fraction	1.01 (0.98 to 1.04)	0.513	1.01 (0.98 to 1.04)	0.642
↓ LV contraction fraction (SV/LVMV)	1.01 (1.00 to 1.02)	0.001	1.01 (1.00 to 1.02)	0.032
↓ LV global function index	1.04 (1.01 to 1.08)	0.024	1.03 (0.99 to 1.07)	0.128
↓ LV Lamé's wall stress	1.00 (1.00 to 1.00)	0.052	1.00 (1.00 to 1.00)	0.258
↓ Pressure-strain loop	1.00 (1.00 to 1.00)	0.234	1.00 (1.00 to 1.00)	0.205
↑ Stroke work	1.00 (1.00 to 1.00)	0.994	1.00 (1.00 to 1.00)	0.990
↓ Stroke work indexed to BSA	1.00 (1.00 to 1.00)	0.479	1.00 (1.00 to 1.00)	0.738
↓ Stroke work indexed to height ^{2.7}	1.00 (1.00 to 1.00)	0.528	1.00 (1.00 to 1.00)	0.600
↓ Stroke work indexed to LV mass	1.01 (1.00 to 1.01)	0.024	1.00 (1.00 to 1.01)	0.111
↓ Global longitudinal strain	1.10 (1.03 to 1.17)	0.003	1.09 (1.02 to 1.16)	0.013
↓ GLASE	1.00 (1.00 to 1.00)	0.348	1.00 (1.00 to 1.00)	0.413
↓ GLASE indexed to BSA	1.00 (1.00 to 1.01)	0.118	1.00 (1.00 to 1.01)	0.281
↓ GLASE indexed to height ^{2.7}	1.01 (1.00 to 1.02)	0.151	1.01 (1.00 to 1.02)	0.256
↓ GLASED	1.38 (1.11 to 1.73)	0.005	1.28 (1.01 to 1.63)	0.038

Model 1 was adjusted for age and sex, and Model 2 was adjusted for age, sex and cardiovascular risk factors (body mass index, hypertension, diabetes mellitus, dyslipidaemia, smoking history, regular alcohol intake, physical activity).

Table S5B. Cox regression analysis of potential prognostic markers for major adverse cardiovascular events in the subgroup with a normal LVEF (>55%)

LV marker	Model 1		Model 2	
	Hazard ratio (95% CI)	P value	Hazard ratio (95% CI)	P value
↑ LV end-diastolic diameter	1.01 (0.99 to 1.03)	0.465	1.01 (0.99 to 1.04)	0.247
↓ LV end-diastolic diameter indexed to BSA	1.04 (1.00 to 1.07)	0.024	1.01 (0.97 to 1.05)	0.658
↑ LV end-diastolic diameter indexed to height ^{2.7}	1.03 (0.97 to 1.09)	0.360	1.02 (0.95 to 1.08)	0.628
↑ LV end-diastolic volume	1.00 (1.00 to 1.00)	0.275	1.00 (1.00 to 1.01)	0.228
↓ LV end-diastolic volume indexed to BSA	1.00 (0.99 to 1.01)	0.731	1.00 (1.00 to 1.01)	0.282
↑ LV end-diastolic volume indexed to height ^{2.7}	1.01 (1.00 to 1.02)	0.137	1.01 (0.99 to 1.02)	0.251
↑ LV mass	1.02 (1.01 to 1.02)	<0.0001	1.02 (1.01 to 1.02)	<0.0001
↑ LV mass indexed to BSA	1.04 (1.03 to 1.05)	<0.0001	1.04 (1.03 to 1.05)	<0.0001
↑ LV mass indexed to height ^{2.7}	1.09 (1.07 to 1.11)	<0.0001	1.09 (1.06 to 1.11)	<0.0001
↑ LV ejection fraction	1.00 (0.98 to 1.02)	0.843	1.01 (0.99 to 1.03)	0.556
↓ LV contraction fraction (SV/LVMV)	1.02 (1.01 to 1.03)	<0.0001	1.02 (1.01 to 1.02)	<0.0001
↓ LV global function index	1.06 (1.03 to 1.09)	<0.0001	1.05 (1.02 to 1.08)	0.0003
↓ LV Lamé's wall stress	1.00 (1.00 to 1.00)	0.012	1.00 (1.00 to 1.00)	0.200
↑ Pressure-strain loop	1.00 (1.00 to 1.00)	0.179	1.00 (1.00 to 1.00)	0.383
↑ Stroke work	1.00 (1.00 to 1.00)	0.0001	1.00 (1.00 to 1.00)	0.002
↑ Stroke work indexed to BSA	1.00 (1.00 to 1.00)	0.002	1.00 (1.00 to 1.00)	0.001
↑ Stroke work indexed to height ^{2.7}	1.00 (1.00 to 1.00)	<0.0001	1.00 (1.00 to 1.00)	0.001
↓ Stroke work indexed to LV mass	1.00 (1.00 to 1.01)	0.011	1.00 (1.00 to 1.01)	0.089
↓ Global longitudinal strain	1.13 (1.08 to 1.18)	<0.0001	1.11 (1.05 to 1.16)	<0.0001
↑ GLASE	1.00 (1.00 to 1.00)	0.116	1.00 (1.00 to 1.00)	0.174
↑ GLASE indexed to BSA	1.00 (1.00 to 1.00)	0.510	1.00 (1.00 to 1.01)	0.178
↑ GLASE indexed to height ^{2.7}	1.01 (1.00 to 1.01)	0.060	1.00 (1.00 to 1.01)	0.160
↓ GLASED	1.39 (1.18 to 1.64)	<0.0001	1.25 (1.06 to 1.48)	0.009

Model 1 was adjusted for age and sex, and Model 2 was adjusted for age, sex and cardiovascular risk factors (body mass index, hypertension, diabetes mellitus, dyslipidaemia, smoking history, regular alcohol intake, physical activity).

Table S5C. Cox regression analysis of potential prognostic markers for heart failure in the subgroup with a normal LVEF (>55%)

LV marker	Model 1		Model 2	
	Hazard ratio (95% CI)	P value	Hazard ratio (95% CI)	P value
↑ LV end-diastolic diameter	1.10 (1.05 to 1.15)	<0.0001	1.08 (1.03 to 1.14)	0.001
↑ LV end-diastolic diameter indexed to BSA	1.00 (0.93 to 1.08)	0.929	1.18 (1.08 to 1.28)	0.0002
↑ LV end-diastolic diameter indexed to height ^{2.7}	1.35 (1.19 to 1.53)	<0.0001	1.25 (1.09 to 1.44)	0.001
↑ LV end-diastolic volume	1.01 (1.01 to 1.02)	<0.0001	1.01 (1.01 to 1.02)	0.0004
↑ LV end-diastolic volume indexed to BSA	1.02 (1.01 to 1.04)	0.002	1.03 (1.02 to 1.04)	<0.0001
↑ LV end-diastolic volume indexed to height ^{2.7}	1.08 (1.06 to 1.11)	<0.0001	1.07 (1.04 to 1.10)	<0.0001
↑ LV mass	1.03 (1.02 to 1.04)	<0.0001	1.02 (1.01 to 1.03)	0.0001
↑ LV mass indexed to BSA	1.06 (1.04 to 1.08)	<0.0001	1.05 (1.03 to 1.07)	<0.0001
↑ LV mass indexed to height ^{2.7}	1.16 (1.12 to 1.20)	<0.0001	1.11 (1.06 to 1.16)	<0.0001
↓ LV ejection fraction	1.01 (0.96 to 1.05)	0.791	1.01 (0.96 to 1.05)	0.762
↓ LV contraction fraction (SV/LVMV)	1.01 (1.00 to 1.02)	0.029	1.00 (0.99 to 1.01)	0.887
↓ LV global function index	1.05 (0.99 to 1.11)	0.103	1.00 (0.94 to 1.06)	0.958
↑ LV Lamé's wall stress	1.00 (1.00 to 1.00)	0.844	1.00 (1.00 to 1.00)	0.249
↓ Pressure-strain loop	1.00 (1.00 to 1.00)	0.989	1.00 (1.00 to 1.00)	0.703
↑ Stroke work	1.00 (1.00 to 1.00)	<0.0001	1.00 (1.00 to 1.00)	0.003
↑ Stroke work indexed to BSA	1.00 (1.00 to 1.00)	0.002	1.00 (1.00 to 1.00)	0.0006
↑ Stroke work indexed to height ^{2.7}	1.00 (1.00 to 1.00)	<0.0001	1.00 (1.00 to 1.00)	0.0005
↓ Stroke work indexed to LV mass	1.00 (1.00 to 1.01)	0.570	1.00 (0.99 to 1.01)	0.595
↓ Global longitudinal strain	1.14 (1.03 to 1.26)	0.011	1.10 (0.99 to 1.22)	0.085
↑ GLASE	1.00 (1.00 to 1.01)	0.010	1.00 (1.00 to 1.01)	0.064
↑ GLASE indexed to BSA	1.01 (1.00 to 1.01)	0.063	1.01 (1.00 to 1.01)	0.028
↑ GLASE indexed to height ^{2.7}	1.02 (1.01 to 1.04)	0.0006	1.02 (1.00 to 1.03)	0.017
↓ GLASED	1.17 (0.81 to 1.68)	0.401	1.03 (0.71 to 1.49)	0.888

Model 1 was adjusted for age and sex, and Model 2 was adjusted for age, sex and cardiovascular risk factors (body mass index, hypertension, diabetes mellitus, dyslipidaemia, smoking history, regular alcohol intake, physical activity).

Table S6. Atrial Fibrillation and GLASED

Variable	AF -ve	AF +ve	P
N(%)	43,636 (96.1%)	1,321 (2.9%)	
GLASED (SD) (kJ/m ³)	2.56 (0.55)	2.44 (0.61)	<0.001

A total of 1321 people (2.9%) were diagnosed with atrial fibrillation (AF) at the time of CMR imaging. The presence of atrial fibrillation was associated with lower GLASED.